

See discussions, stats, and author profiles for this publication at: <https://www.researchgate.net/publication/268787841>

Synthesis and Biological Evaluation of Novel Sigma-1 Receptor Antagonists Based on Pyrimidine Scaffold As Agents for Treating Neuropathic Pain

ARTICLE in JOURNAL OF MEDICINAL CHEMISTRY · NOVEMBER 2014

Impact Factor: 5.45 · DOI: 10.1021/jm501207r · Source: PubMed

CITATION

1

READS

29

11 AUTHORS, INCLUDING:



Yu Lan

Wuhan University

5 PUBLICATIONS 5 CITATIONS

SEE PROFILE



xu Xiangqing

Huazhong University of Science and Technology

13 PUBLICATIONS 50 CITATIONS

SEE PROFILE



Xin Liu

Huazhong University of Science and Technology

76 PUBLICATIONS 1,127 CITATIONS

SEE PROFILE

Synthesis and Biological Evaluation of Novel Sigma-1 Receptor Antagonists Based on Pyrimidine Scaffold As Agents for Treating Neuropathic Pain

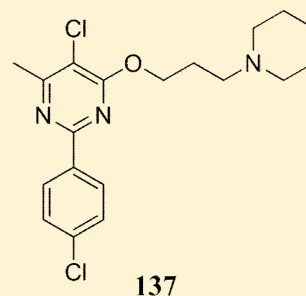
Yu Lan,^{†,§} Yin Chen,^{‡,§} Xudong Cao,[†] Juecheng Zhang,[†] Jie Wang,[†] Xiangqing Xu,[‡] Yinli Qiu,[‡] Tan Zhang,[‡] Xin Liu,[†] Bi-Feng Liu,[†] and Guisen Zhang^{*,†,‡}

[†]Systems Biology Theme, Department of Biomedical Engineering, College of Life Science and Technology, Huazhong University of Science and Technology, Wuhan 430074, China

[‡]Jiangsu Nhwa Pharmaceutical Co., Ltd., 69 Democratic South Road, Xuzhou, Jiangsu 221116, China

S Supporting Information

ABSTRACT: The discovery and synthesis of a new series of pyrimidines as potent sigma-1 receptor (σ_1 R) antagonists, associated with pharmacological antineuropathic pain activity, are the focus of this article. The new compounds were evaluated *in vitro* in σ -1 and σ -2 receptor binding assays. The nature of the pyrimidine scaffold was crucial for activity, and a basic amine was shown to be necessary according to the known pharmacophoric model. The most promising derivative was 5-chloro-2-(4-chlorophenyl)-4-methyl-6-(3-(piperidin-1-yl)propoxy)pyrimidine (**137**), which exhibited a high binding affinity to σ_1 R receptor ($K_i \sigma_1 = 1.06$ nM) and good σ -1/2 selectivity (1344-fold). *In vivo* tests, compound **137** exerted dose-dependent antinociceptive effects in mice formalin model and rats CCI models of neuropathic pain. In addition, no motor impairments were found in rotarod tests; acceptable pharmacokinetic properties were also noted. These data suggest compound **137** may constitute a novel class of drugs for the treatment of neuropathic pain.



137

In vitro: $K_i \sigma_1 = 1.06$ nmol; $K_i \sigma_2 = 1425$ nmol; Pharmacokinetic: $t_{1/2} = 3.81$ h; F% = 75.1

■ INTRODUCTION

Neuropathic pain is widely recognized as one of the most difficult clinical syndromes, which affects 8% of the population and is considerably costly for the health care system and devastating to the people who experience it.^{1,2} Although progress has been made from basic science and clinical research and preclinical neuropathic pain models have facilitated identification of several promising targets, innovations in the field of pain in recent years are lacking. Available therapies often provide incomplete pain relief and treatment-related side effects are common; thus neuropathic pain management remains a challenge.³

Various guidelines have been established for the pharmacological management of neuropathic pain.^{4–6} Although differing in detail, the guidelines are generally consistent.⁷ Medications recommended as first-line treatments for neuropathic pain include antidepressants (such as tricyclic antidepressants, TCA, and dual reuptake inhibitors of both serotonin and norepinephrine), calcium channel α_2 - δ ligands (gabapentin and pregabalin), and topical lidocaine. These medications are very effective in reducing pain in several neuropathic pain disorders, but treatment may be compromised and outweighed by its side effects. Opioid analgesics can alleviate nociceptive and neuropathic pain with a mean decrease in pain intensity, comparable with TCA and gabapentin/pregabalin. Regarding their long-term safety, opioid-induced hyperalgesia and the risk

of addiction relative to the first-line medications, opioid analgesics are recommended typically for patients who have not responded to first-line medications. Several medications are generally used as third-line treatments because of weak efficacy, discrepant results, or safety concerns, including anticonvulsants, NMDA receptor antagonists, and topical capsaicin. Thus, neuropathic pain analgesics with novel mechanisms of action that improve the efficacy of existing therapies and reduce unwanted effects are needed.^{8–10}

The sigma receptors (σ R) were first discovered in 1976¹¹ and mischaracterized originally as a new class of opioid receptors. Later, sigma receptors were confused with the PCP/NMDA glutamate receptor complex because of nonselective ligands.^{12,13} Currently, sigma receptors are considered unique proteins without homology to opioid receptors or other mammalian proteins.¹⁴ Pharmacological studies and biochemical analyses have identified two distinct subtypes of sigma receptor, termed the sigma-1 (σ_1) and sigma-2 (σ_2) receptors.^{15,16} The σ_1 R has been purified and cloned and encodes a protein of 223 amino acids with a molecular weight of ~ 24 kDa.¹⁷ Investigations have suggested that the σ_1 R plays an important role in central nervous system (CNS) function.¹⁸ This protein acts as a unique ligand-regulated molecular

Received: August 6, 2014

Published: November 24, 2014

chaperone that modulates the activity of different proteins such as *N*-methyl-D-aspartic (NMDA)¹⁹ receptors and several ion channels.^{20–22} The σ_2 R has not been characterized as well as the σ_1 R, and cloning of the σ_2 R has not been reported. Recently, the σ_2 R was shown to be involved in cellular proliferation and cell death, and radiolabeled ligands acting on σ_2 R have been used for tumor imaging techniques (i.e., positron emission tomography, PET). Numerous studies suggest that the σ_2 R is an excellent biomarker and a promising therapeutic target for the treatment of cancer.^{23,24} Due to their different pharmacological functions, selectivity between the σ_1 R and σ_2 R is desirable.

To date, selective σ_1 R ligands have not been introduced to the market, but many of the compounds have been tested in clinical studies as antidepressants,²⁵ antipsychotics,²⁶ treatments for drug abuse,²⁷ and learning/memory enhancers.²⁸ Moreover, numerous groups have studied the potential role of the σ_1 R in pain management, especially neuropathic pain.²⁹ Since the 1990s, the σ_1 R has been known to modulate opioid analgesia,^{30–32} and recently, the relationship between the μ -opioid and σ_1 R was shown to involve a direct physical interaction.³³ Treatment with σ_1 R antagonists or σ_1 R antisense oligodeoxynucleotides enhanced the antinociceptive effect induced by morphine and other μ -opioid receptor agonists in the acute nociceptive test, while σ_1 R agonists reduced the analgesic response elicited by opioids.^{34,35} The σ_1 R also plays a nociceptive role in the absence of opioids, as shown in studies using σ_1 R knockout mice and certain behavioral models involving pain sensitization pathways. Mice lacking σ_1 R were unable to develop completely the two phases of formalin-induced paw licking/biting behavior³⁶ and showed no mechanical hypersensitivity following capsaicin sensitization.³⁷ In an animal model of neuropathic pain, cold and mechanical hypersensitivity were strongly attenuated in σ_1 R knockout mice treated with paclitaxel³⁸ or exposed to partial sciatic nerve ligation.³⁹ Pharmacological antagonism of the σ_1 R produced similar results. Haloperidol and its metabolites I and II, which have an affinity for the σ_1 R, inhibited formalin-induced pain⁴⁰ and capsaicin-induced sensitization in wild-type mice.⁴¹ The recently described σ_1 R antagonists, S1RA, with high affinity to σ_1 receptors ($K_i = 17$ nM) and excellent selectivity ratio ($\sigma_2/\sigma_1 > 550$), are currently undergoing phase II clinical trials for treatment of neuropathic pain^{42,43} (Figure 1).

Our interest has focused on the development of novel ligands with high affinity to the σ_1 R and selectivity over the σ_2 R

subtype.⁴⁴ Using a three-dimensional (3D) pharmacophore model of σ_1 R antagonists and virtual screening program, we identified a new series of compounds based on pyrimidine scaffold. Herein, we report the synthesis and investigated the behavior of pyrimidine derivatives as novel and potent antineuropathic analgesics. The compounds were subjected to preliminary pharmacological evaluation to determine their affinities to the σ_1 R and σ_2 R. Their structure–activity relationships (SARs) for the σ_1 R and σ_2 R were associated with variation in the basic amino moieties and substituents on the pyrimidine scaffold. Among the derivatives prepared, compound 137 exhibited a high binding affinity to σ_1 R ($K_i \sigma_1 = 1.06$ nM), good σ_1 R/ σ_2 R selectivity (1344-fold), and was identified as a σ_1 R antagonist. Weak affinity to hERG channels indicated that compound 137 had a low incidence of cardiac toxicity. In addition, compound 137 inhibited dose-dependent antinociceptive effects in the mouse formalin-induced pain model and rat chronic constriction injury (CCI) model. Motor impairments were not found in rotarod tests at analgesic doses, and acceptable pharmacokinetic properties were observed. On the basis of these properties, compound 137 may be considered a novel class of drugs for the treatment of neuropathic pain.

MOLECULAR DESIGN

As the lack of three-dimensional protein structure of a σ_1 receptor,¹⁸ the main focus of current efforts toward the development of a new σ_1 R ligand is concentrated on structure-based ligand design. In this work, Discovery Studio 2.5 software (DS) was utilized to build and validate pharmacophore model. 3D pharmacophore hypotheses were built based on a set of known diverse σ_1 R antagonists. The best pharmacophore model, which identified compounds with an associated correlation coefficient of 0.94027 between the experimental and estimated K_i value, consisted of four pharmacophoric feature: HBA (green), Hydrophob_aromatic (blue), Hydrophobic (light blue), and PosIonizable (red), as shown in Figure 2A. Detailed information about 3D pharmacophore model generation can be found in the Support Information.

On the basis of the preliminary founding of virtual screening by this 3D pharmacophore model and analysis of hits identification, we got the pyrimidine scaffold and design a series of compounds (Figure 2B). In detail, the chemical structures of these pyrimidine derivatives were designed according to the following rationale: we changed the distance between the pyrimidine ring and basic amino moiety (carbon chain linker) to validate the requirement of the pharmacophoric model, tested various basic amino moieties to fit the PosIonizable and Hydrophobic feature (NR_1R_2), took different substitution on the 4- and 5-positions of the pyrimidine ring (R_3 and R_4), and replaced the 2-phenyl group of pyrimidine by an aromatic ring or small alkyl group (R_5) to find the best conformational fitting to the receptor.

CHEMISTRY

The synthesis of the new compounds was accomplished using different routes, as shown in Schemes 1–5.

As depicted in Scheme 1, phenyl aminoalkoxy pyrimidine derivatives 8 and 14–34 were obtained using two alternative procedures. The key intermediate 6-methyl-2-phenylpyrimidin-4-ol 7 was prepared using a one-step procedure from benzimidamide 5, which was cyclized with a moderate yield of ethyl 3-oxobutanoate 6. Depending on the substitution

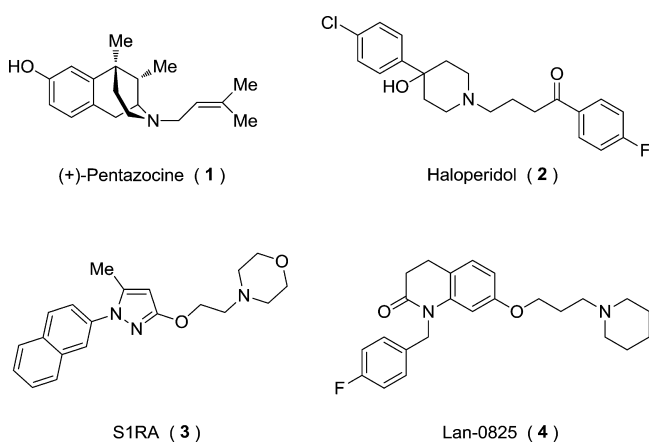


Figure 1. Representative σ_1 receptor ligands.

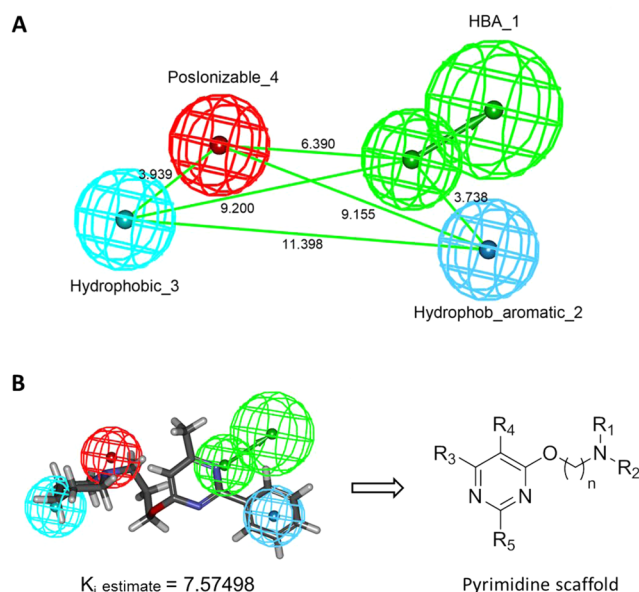
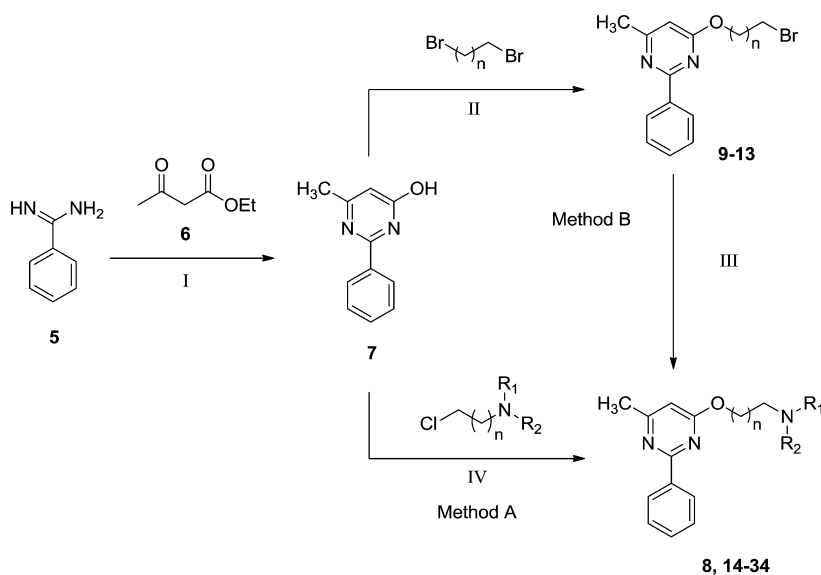


Figure 2. (A) The 3D-QSAR pharmacophore model of σ -1R antagonist. The model is constituted with four pharmacophore features: HBA, green; Hydrophob aromatic, blue; Hydrophobic, light blue; and Poslonizable, red. (B) The virtual screening result and molecular design of pyrimidine scaffold by this 3D-QSAR model.

pattern, the final compounds **8** and **14–34** were prepared using method A or the two-step procedure, method B (Tables 1, 2). In method A, **7** was reacted with commercially available chloroalkylamine under a basic condition to obtain a good yield of compound **8**. Method B involved standard alkylation with 1,*n*-dibromoalkanes to produce **9–13**, and reaction with the corresponding amines under mild basic conditions resulted in moderate yields of the final compounds **14–34**. The general synthetic methods for phenyl aminoalkoxy pyrimidine derivatives **8** and **14–34** (methods A and B) are described in the Experimental Section.

Scheme 1^a



^aReagents and conditions: (I) *t*-BuOK, MeOH, reflux; (II) Br(CH₂)_nBr, K₂CO₃, acetone, reflux; (III) HNR₁R₂, Cs₂CO₃, acetonitrile, reflux; (IV) K₂CO₃, KI, acetonitrile, reflux;

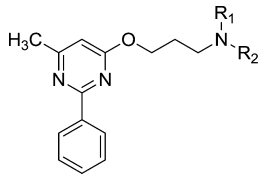
Table 1. Binding Affinities for the σ_1 and σ_2 Receptor of Compounds **8**, **14–18**, **36**, and **38**

compd	Z	K_i σ_1 (nM) ^a	K_i σ_2 (nM) ^b	selectivity (σ_2/σ_1)
8	(CH ₂) ₂	>2000	>2000	
14	(CH ₂) ₃	36.3 ± 4.8 ^c	949 ± 65	26.1
15	(CH ₂) ₄	95.2 ± 7.6	1072 ± 82	11.2
16	(CH ₂) ₅	389 ± 63	>2000	
17	(CH ₂) ₆	>2000	>2000	
18	CH ₂ CH=C HCH ₂	116 ± 9.4	1451 ± 82	12.5
36	(CH ₂) ₂ O(CH ₂) ₂	422 ± 73	1924 ± 107	4.6
38	CH ₂ CHOHCH ₂	486 ± 85	1644 ± 124	3.4

^aAffinities were determined in guinea pig brain using [³H]-(+)-pentazocine. ^bAffinities were determined in guinea pig brain using [³H]-DTG in the presence of (+)-SKF-10047 to block σ -1 receptors. ^cThe values are means ± SEM of three experiments performed in duplicate.

Elongated analogues **36** and **38** were obtained starting from 6-methyl-2-phenylpyrimidin-4-ol **7**, as shown in Scheme 2. Alkylation of **7** with 1-bromo-2-(bromoethoxy)ethane under basic conditions produced the monosubstituted **35**, which was reacted with morpholine to afford compound **36**. Hydroxyl derivative **38** was prepared by treatment of **7** with 2-(chloromethyl)oxirane under basic conditions, followed by ring-opening with morpholine.

The route depicted in Scheme 3 was used for the preparation of substituted pyrimidine scaffold compounds **69–78** and **79–88**. The intermediates **49–58** were obtained using the cyclization procedure with benzimidamide **5**, which was reacted

Table 2. Binding Affinities for the σ_1 and σ_2 Receptors of Compounds 14 and 19–34


Compound	NR ₁ R ₂	K _i σ_1 (nM) ^a	K _i σ_2 (nM) ^b	Selectivity (σ_2/σ_1)
14		36.3 ± 4.8 ^c	949 ± 65	26.1
19		11.8 ± 2.6	1051 ± 87	89.1
20		16.7 ± 5.2	1416 ± 73	84.7
21		30.2 ± 7.4	1662 ± 103	55.0
22		377 ± 39	>2000	----
23		462 ± 82	1763 ± 204	3.8
24		319 ± 68	1492 ± 122	4.7
25		151 ± 19	1212 ± 138	8.0
26		22.7 ± 4.1	1325 ± 96	58.3
27		30.6 ± 8.3	1179 ± 88	38.5
28		18.7 ± 4.9	1295 ± 104	69.2
29		>2000	>2000	----
30		>2000	>2000	----
31		13.6 ± 3.1	1253 ± 178	92.1
32		82.3 ± 10.7	>2000	----
33		47.1 ± 8.4	1317 ± 106	28.0
34		38.8 ± 6.3	1069 ± 89	27.5

^aAffinities were determined in guinea pig brain using [³H]-(+)-pentazocine. ^bAffinities were determined in guinea pig brain using [³H]-DTG in the presence of (+)-SKF-10047 to block σ_1 receptors. ^cThe values are means ± SEM of three experiments performed in duplicate.

with various substituted ethyl 3-oxobutanoates 39–48, depending on the substitution pattern of the final pyrimidine. Next, standard alkylation with 1,3-dibromopropane was conducted to

produce 59–68, and then reaction with the piperidine or pyrrolidine afforded the final compounds 69–78 and 79–88, respectively, with moderate yields (Table 3).

6,7-Dihydro-5H-cyclopenta[d]pyrimidines 94–95 and 5,6,7,8-tetrahydroquinazoline 97–98 (Scheme 4 and Table 4) were prepared by reaction of 5 with ethyl 2-oxocyclopentanecarboxylate or 2-oxocyclohexanecarboxylate to obtain intermediates 91 and 92, which were subsequently alkylated with 1,3-dibromopropane and reacted with piperidine or pyrrolidine, under conditions similar to those used for substituted pyrimidine derivatives.

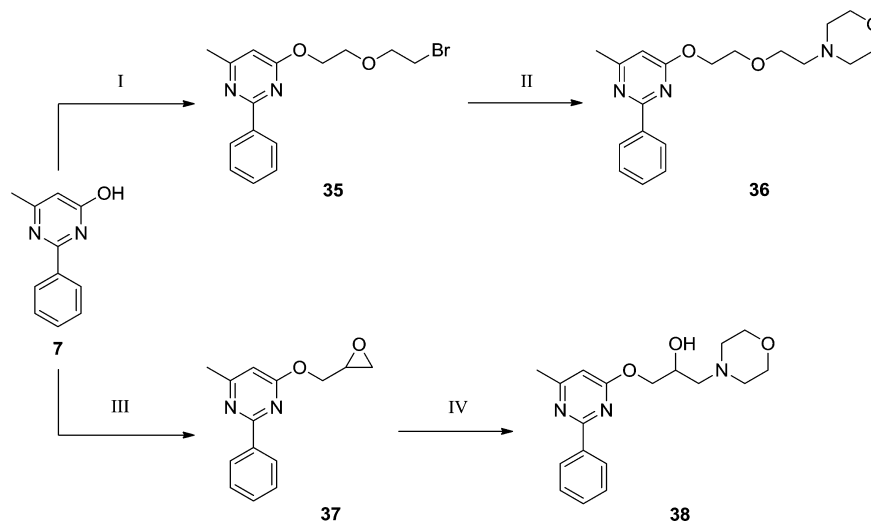
The syntheses of the 2-substituted 5-chloro-4-methyl-6-aminoalkoxy pyrimidine derivatives 132–142 were accomplished by the corresponding aryl- or alkyl- amidine 99–109 that were reacted with ethyl 2-chloro-3-oxobutanoate 48, followed by alkylation with 1,3-dibromopropane and reaction with piperidine (Scheme 5 and Table 5). The nonsubstituted 5-chloro-4-methyl-6-aminoalkoxy pyrimidine, intermediate 118, which is soluble in water, was purified using flash chromatography.

RESULTS AND DISCUSSION

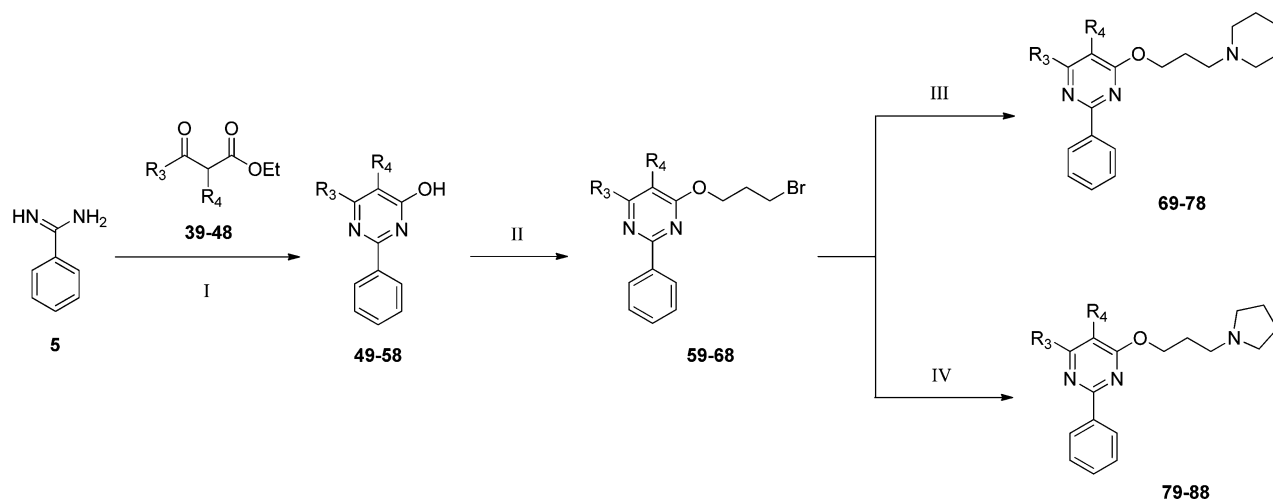
Structure–Activity Relationships. The design of the new series of pyrimidines derivatives was based on the known pharmacophoric features of σ_1 R ligands. As recently summarized by Glennon et al., σ_1 R inhibitors should contain a basic amino group and no less than two hydrophobic regions at specified distances, 2.5–3.9 and 6–10 Å from the amino group^{45,46} (Figure 3A). Compounds of the general structure (Figure 3B) were designed in which the pyrimidine acted as an important scaffold and various groups added according to these pharmacophoric requirements; some variations were also considered.

Effect of the Distance between the Pyrimidine Ring and the Basic Amino Moiety. In this study, our initial focus was to investigate the effect of different chain lengths on affinities to σ_1 R and σ_2 R (Table 1, compounds 8, 14–34, 36, and 38). The morpholine group was used because of its frequent appearance in σ_1 R ligands, such as S1RA. At position 2 of the pyrimidine ring, a simple nonsubstituted phenyl was selected to meet the requirement of the pharmacophoric model.

Initially, the two-carbon linker compound 8 was prepared but did not activate either receptor; apparently the linker was too short. Increasing the linker with only one carbon atom (14) demonstrated binding affinity and selectivity for the σ_1 R over the σ_2 R ($K_i \sigma_1 = 36.3$ nM and $K_i \sigma_2 = 949$ nM). Further elongation of the straight carbon linker between the pyrimidine scaffold and morpholine moiety provided derivatives 15–16, which had lower σ_1 R and σ_2 R affinities than their propylene counterparts. Derivatives of a six-atom spacer, compound 17, did not bind either receptor, suggesting the distance was too large for the binding site. Compared to compound 15, replacing the single bond with a trans double bond (18) did not promote affinity to the σ_1/σ_2 receptor. A five-atom linker with an intercalated oxygen atom (36) maintained the potency for both receptors as compound 16. The introduction of a hydroxyl group in the linker (38) resulted in decreased potency for both receptors, suggesting that polar groups are not preferred in this region. Taken together, the data indicated that the distance between the pyrimidine and basic amino group affected significantly the potency of both receptors; three-carbon chain length (14) was the most preferred and so was further investigated.

Scheme 2^a

^aReagents and conditions: (I) $\text{Br}(\text{CH}_2)_2\text{O}(\text{CH}_2)_2\text{Br}$, K_2CO_3 , KI, acetone, reflux; (II) morpholine, Cs_2CO_3 , acetonitrile, reflux; (III) 2-(chloromethyl)oxirane, K_2CO_3 , KI, acetone, reflux; (IV) morpholine, MeOH, reflux.

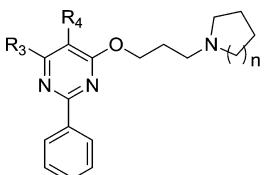
Scheme 3^a

^aReagents and conditions: (I) *t*-BuOK, MeOH, reflux; (II) $\text{Br}(\text{CH}_2)_3\text{Br}$, K_2CO_3 , acetone, reflux; (III) piperidine, Cs_2CO_3 , acetonitrile, reflux; (IV) pyrrolidine, Cs_2CO_3 , acetonitrile, reflux.

Effect of the Basic Amino Moiety for Different Amino Groups. After determining the scaffold of the phenyl pyrimidine derivatives, the effect of various basic amino moieties was investigated by synthesizing variations of compound 14. As shown in Table 2, we selected piperidine, 4-methylpiperidine, 3,5-dimethylpiperidine, and 2,2,6,6-tetramethylpiperidine (compounds 19–22) to replace the morpholine moiety. The substitution of morpholine with piperidine analogues resulted in compound 19, which showed significantly improved $\sigma_1\text{R}$ binding affinity and selectivity ($K_i \sigma_1 = 11.8 \text{ nM}$ and $K_i \sigma_2 = 1051 \text{ nM}$). The improvement was possibly due to the greater hydrophobicity of the piperidine moiety, which was closer in similarity to Glennon's pharmacophoric $\sigma_1\text{R}$ model.^{45,46} Increasing the hydrophobic ability of piperidinyl by adding a methyl group on the ring (20–21) did not enhance the receptor's binding affinity, which suggested that the space in this region was limited. The compound with 2,2,6,6-tetramethylpiperidine (22) showed weak affinity ($K_i \sigma_1 = 377$

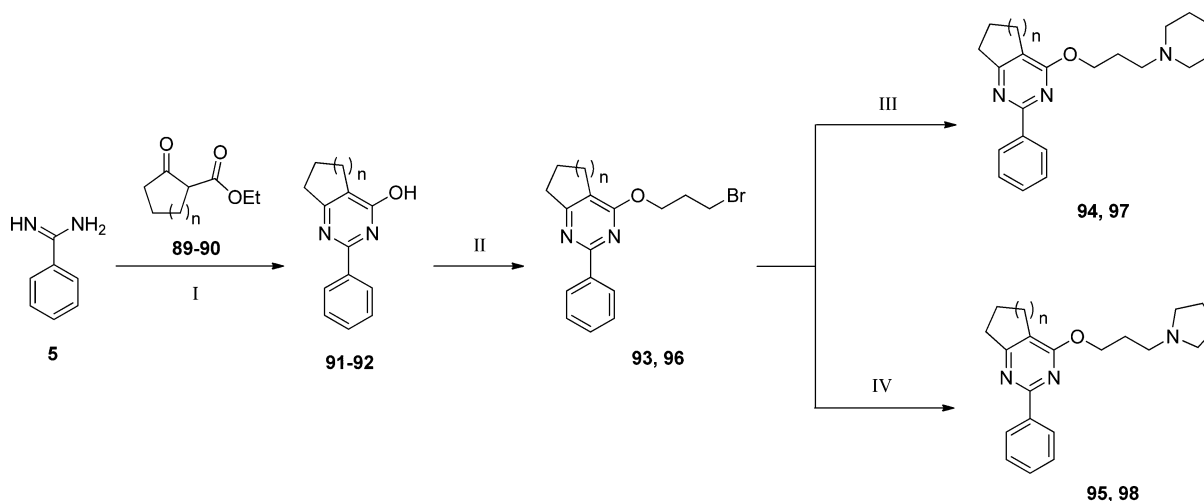
nM and $K_i \sigma_2 > 2000 \text{ nM}$) to both receptors, mainly because the four methyls formed a strong steric hindrance around the N atom, affecting the ligand–receptor interaction. Substituting the oxygen atom of the morpholino with a hydroxyl group or carbonyl group (23–24) decreased greatly the affinity to both the $\sigma_1\text{R}$ and $\sigma_2\text{R}$, which suggested the polar groups were not conducive to $\sigma_1\text{R}$ or $\sigma_2\text{R}$ binding in this position.

Changing the oxygen atom in the morpholino group to a N atom produced the piperazine derivative, compound 25, which showed a weak receptor affinity ($K_i \sigma_1 = 151 \text{ nM}$ and $K_i \sigma_2 = 1212 \text{ nM}$) and may be due to the hydrophilic property of piperazine. Substituting the hydrogen in piperazine with small alkyl groups improved the hydrophobic property and resulted in the potent and selective compounds 26–27 and in the larger diazepane derivative, compound 28 ($K_i \sigma_1 = 18.7 \text{ nM}$ and $K_i \sigma_2 = 1295 \text{ nM}$). However, substituting with large groups, such as *t*-butyloxycarbonyl (29) or phenyl (30), was not tolerated by either the $\sigma_1\text{R}$ or $\sigma_2\text{R}$.

Table 3. Binding Affinities for the σ_1 and σ_2 Receptor of Compounds 19, 31, and 69–88


compd	n	R ₃	R ₄	K _i σ_1 (nM) ^a	K _i σ_2 (nM) ^b	selectivity (σ_2/σ_1)
19	2	CH ₃	H	11.8 ± 2.6 ^c	1051 ± 87	89.1
69	2	CH ₂ CH ₃	H	20.5 ± 3.3	1141 ± 97	55.6
70	2	(CH ₂) ₂ CH ₃	H	34.9 ± 6.1	1456 ± 127	41.7
71	2	CH(CH ₃) ₂	H	188 ± 25	1836 ± 232	9.7
72	2	OCH ₃	H	19.3 ± 4.6	892 ± 77	46.2
73	2	CF ₃	H	27.6 ± 5.9	1327 ± 101	48.0
74	2	cyclopropyl	H	253 ± 46	>2000	
75	2	phenyl	H	966 ± 92	>2000	
76	2	CH ₃	CH ₃	9.51 ± 1.3	1221 ± 104	128
77	2	CH ₃	F	3.75 ± 0.4	1361 ± 119	363
78	2	CH ₃	Cl	2.33 ± 0.6	1649 ± 119	708
31	1	CH ₃	H	13.6 ± 3.1	1253 ± 78	92.1
79	1	CH ₂ CH ₃	H	22.4 ± 4.1	1429 ± 133	63.8
80	1	(CH ₂) ₂ CH ₃	H	38.9 ± 7.6	1396 ± 121	35.8
81	1	CH(CH ₃) ₂	H	218 ± 55	1092 ± 172	5.0
82	1	OCH ₃	H	19.3 ± 4.6	892 ± 77	46.2
83	1	CF ₃	H	27.6 ± 5.9	1327 ± 101	48.0
84	1	cyclopropyl	H	278 ± 51	>2000	
85	1	phenyl	H	735 ± 108	>2000	
86	1	CH ₃	CH ₃	11.4 ± 1.2	1279 ± 173	112
87	1	CH ₃	F	3.51 ± 0.7	1194 ± 97	340
88	1	CH ₃	Cl	4.02 ± 0.6	1684 ± 131	419

^aAffinities were determined in guinea pig brain using [³H]-(+)-pentazocine. ^bAffinities were determined in guinea pig brain using [³H]-DTG in the presence of (+)-SKF-10047 to block sigma-1 receptors. ^cThe values are means ± SEM of three experiments performed in duplicate.

Scheme 4^a

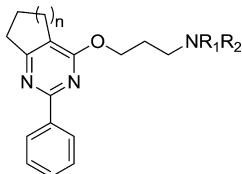
^aReagents and conditions: (I) *t*-BuOK, MeOH, reflux; (II) Br(CH₂)₃Br, K₂CO₃, acetone, reflux; (III) piperidine, Cs₂CO₃, acetonitrile, reflux; (IV) pyrrolidine, Cs₂CO₃, acetonitrile, reflux.

Smaller pyrrolidine analogues showed good potency and maintained the selectivity (27, K_i σ_1 = 13.6 nM and K_i σ_2 = 1253 nM). Open-chain amines (32–34) retained some activity (albeit less than compounds 19 and 31) and exhibited lower selectivity.

Effects of Substitution on the 4- and 5-Positions of the Pyrimidine Ring. The piperidinyl and pyrrolidinyl groups

emerged as the best two amino moieties in receptor binding affinity and selectivity, and the three-carbon linker was selected as the proper distance to match the pharmacophoric requirement. Thus, compounds 19 and 31 were selected for further investigation of the SAR.

We first explored the effects of replacing the methyl (R₃) with other substituents (Table 3, 69–75, 79–85). The affinities

Table 4. Binding Affinities for the σ_1 and σ_2 Receptor of Compounds 94–95, 97, and 98


Compound	n	NR ₁ R ₂	K _i σ_1 (nM) ^a	K _i σ_2 (nM) ^b	Selectivity (σ_2/σ_1)
94	1		44.2 ± 8.2 °	1626 ± 187	36.7
95	1		58.9 ± 7.6	1896 ± 227	32.1
97	2		138.5 ± 20	>2000	----
98	2		111.8 ± 16	1916 ± 227	17.1

^aAffinities were determined in guinea pig brain using [³H]-(+)-pentazocine. ^bAffinities were determined in guinea pig brain using [³H]-DTG in the presence of (+)-SKF-10047 to block sigma-1 receptors. °The values are means ± SEM of three experiments performed in duplicate.

of compounds 69–70 and 79–80 vs compounds 19 and 31 to σ_1 R and σ_2 R decreased as a result of the additional group size or hydrophobicity. The substitution of a methyl group with isopropyl (71, 81), cyclopropyl (74, 84), and phenyl (75, 85) groups produced a significant decrease in the affinities for the receptors, which confirmed the above-stated conclusion. On the basis of these results, the modification of the group in the 4-position (R₃) of the pyrimidine produced analogues in the following order of σ_1 R affinities: methyl > ethyl > isopropyl > *n*-propyl > cyclopropyl > phenyl. The electron-withdrawing groups, methoxyl (72, 82) and trifluoromethyl (73, 83), showed good potency for the σ_1 R, but weaker selectivity than the methyl group.

Introduction to the 5-position (R₄) in the pyrimidine scaffold with a small group (76, K_i σ_1 = 9.51 nM and K_i σ_2 = 1221 nM; 86, K_i σ_1 = 11.4 nM and K_i σ_2 = 1279 nM) led to good affinity for the σ_1 R and maintained selectivity to the σ_2 R. Therefore, we continued the investigation by introducing other substituents at this position. Introducing halogens such as fluorine (77, 87) and chlorine (78, 88) showed moderate affinities to the σ_1 R and increased selectivity to the σ_2 R. Notably, compound 78, with chlorine in the 5-position of the pyrimidine and piperidinyl basic moiety, showed significantly higher binding

affinity to σ_1 R (K_i σ_1 = 2.33 nM) and σ_1/σ_2 selectivity (708-fold) compared with pyrrolidinyl analogues (88). Fluorosubstituted analogue 77 showed less selectivity (363-fold), possibly due to the hydrogen bonding effect of the fluorine atom, which was not preferred in this position.

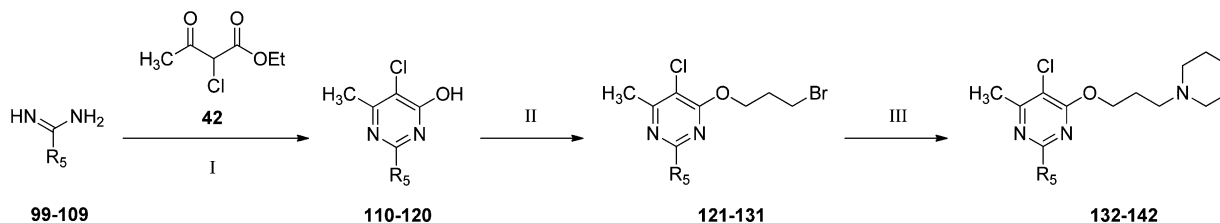
To better explain the SAR of substitution on the pyrimidine ring, ring derivatives connecting the 4- or 5-positions were prepared (Table 4) as 6,7-dihydro-5H-cyclopenta[*d*]-pyrimidines (94–95) and 5,6,7,8-tetrahydroquinazolins (97–98), respectively. The binding affinities of these compounds showed the five-membered ring on pyrimidine could maintain the affinity to the σ_1 R and preferential selectivity with the piperidinyl moiety (94, K_i σ_1 = 44.2 nM, K_i σ_2 = 1626 nM). A six-membered ring in the same position resulted in loss of activity, possibly due to the larger ring size hindering receptor binding.

Effect of Replacing the Phenyl Group on the 2-Position of the Pyrimidine Ring (78) with Another Aromatic Ring. Compound 78 exhibited significant affinity to the σ_1 R and σ_1/σ_2 selectivity and was thus used for further investigation of the effect of various aromatic rings (Table 5, 132–142). The nature of the aromatic group on the 2-position was important for activity and selection. Either introducing an electron-donating group (methyl) or electron-withdrawing group (methoxyl and trifluoromethyl) would increase activity, but halogens, such as fluorine (135, K_i σ_1 = 1.14 nM, K_i σ_2 = 1329 nM) and chlorine (137, K_i σ_1 = 1.06 nM, K_i σ_2 = 1425 nM), showed high affinity to σ_1 R and good selectivity to σ_2 R. The 3,4-difluorophenyl (136) group maintained the receptor-binding profile, but 3,4-dichlorophenyl (138) and 2-naphthyl (139) were not conducive to σ_1 or σ_2 receptor binding in this position. Replacing the aromatic group at the 2-position with hydrogen (140) or a small alkyl such as methyl (141) resulted in a marked reduction in potency. Cyclopropyl (142, K_i σ_1 = 39.5 nM, K_i σ_2 = 1328 nM) only maintained partial potency and selectivity, thus suggesting the importance of an aromatic ring in this position.

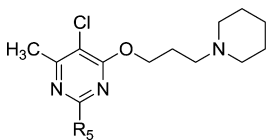
Human Ether-a-go-go-Related Gene (hERG) KC Channel. Human ether-a-go-go-related gene (hERG) channel blockade is an important predictor of cardiac toxicity. The compounds with K_i σ_1 < 5 nM and selectivity >400-fold were subjected to a hERG patch-clamp assay⁴⁷ as shown in Table 6. In this experiment, a cutoff value of IC₅₀ > 5 μ M was used.

Acute Toxicity. After considering the above-mentioned results, the compounds that exhibited high affinity to σ_1 R and good selectivity to σ_2 R, with low affinity for hERG, were assayed for acute toxicity. The acute toxicities of compounds were evaluated in terms of LD₅₀ values (Table 6). Compound 137 showed a good profile even at the highest dose tested (LD₅₀ > 2000 mg/kg).

Scheme 5^a



^aReagents and conditions: (I) *t*-BuOK, MeOH, reflux; (II) Br(CH₂)₃Br, K₂CO₃, acetone, reflux; (III) piperidine, Cs₂CO₃, acetonitrile, reflux.

Table 5. Binding Affinities for the σ_1 and σ_2 Receptor of Compounds 78 and 132–142


compd	R ₅	K _i σ_1 (nM) ^a	K _i σ_2 (nM) ^b	selectivity (σ_2/σ_1)
78	phenyl	2.33 ± 0.6 ^c	1649 ± 119	708
132	4-methylphenyl	1.96 ± 0.7	1554 ± 92	792
133	4-methoxyphenyl	3.88 ± 1.0	1288 ± 76	332
134	4-(trifluoromethyl)phenyl	4.42 ± 1.4	1776 ± 135	402
135	4-fluorophenyl	1.14 ± 0.2	1329 ± 202	1165
136	3,4-difluorophenyl	0.97 ± 0.1	943 ± 156	973
137	4-chlorophenyl	1.06 ± 0.2	1425 ± 139	1344
138	3,4-dichlorophenyl	89.8 ± 13	>2000	
139	2-naphthyl	102 ± 19	>2000	
140	H	187 ± 14	1104 ± 88	5.9
141	CH ₃	58.8 ± 7.2	1081 ± 63	18.4
142	cyclopropyl	39.5 ± 6.8	1328 ± 104	33.6

^aAffinities were determined in guinea pig brain using [³H]-(+)-pentazocine. ^bAffinities were determined in guinea pig brain using [³H]-DTG in the presence of (+)-SKF-10047 to block σ_1 receptors. ^cThe values are means ± SEM of three experiments performed in duplicate.

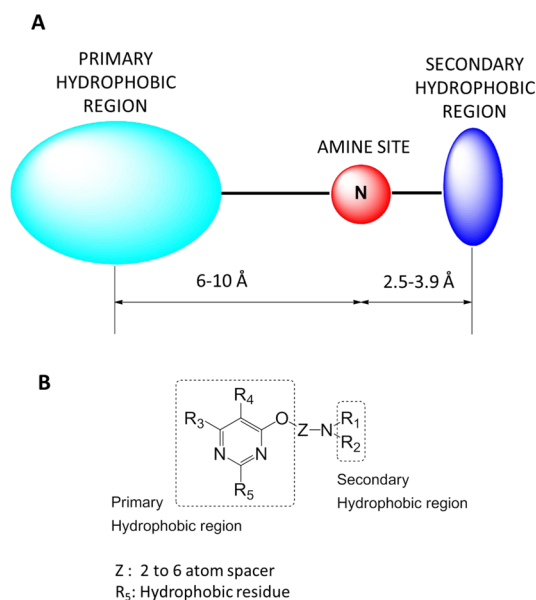


Figure 3. Glennon's pharmacophoric σ_1 receptor model (A) and general structure of the new pyrimidine derivative (B).

Table 6. Additional Data for Compounds Complying with K_i σ_1 < 5 nmol and Selectivity >400-Fold

compd	hERGIC ₅₀ (μmol)	LD ₅₀ (mg/kg)
78	0.28	439.5 (361.0–534.9)
88	3.76	>2000
132	0.95	1684.2 (1500.4–1892.1)
134	2.61	377.3 (298.8–476.5)
135	1.54	884.5 (755.7–1162.7)
136	1.40	584.8 (455.7–750.5)
137	6.98	>2000

Functional Profile of σ_1 Receptor. The phenytoin-media shift on σ_1 R ligand affinity and FRET based biosensor of σ_1 R ligand were mainly used to categorize compounds into agonists and antagonists recently.⁴⁸ In these work, the functional activity of compounds with high σ_1 receptor binding affinity and

selectivity to the σ_1 R over the σ_2 R was evaluated using phenytoin, a low-potency allosteric modulator of the σ_1 receptor. Phenytoin shifts σ_1 R agonists to significantly higher affinities (K_i ratios without phenytoin vs with phenytoin >1), while σ_1 R antagonists show no effect or a very little effect on lowering the affinity values (K_i ratios without phenytoin vs with phenytoin ≤1). Compound 137 produced a small shift, lowering the affinity when incubated in the presence of phenytoin (K_i ratios without phenytoin vs with phenytoin = 0.87), which exhibited antagonist properties on the σ_1 receptor.

Formalin-Induced Nociceptive Behavior. Because of the marked effects on the σ_1 R and σ_2 R with its antagonist property and good safety profile, compound 137 was selected as a promising candidate and subjected to further pharmacological evaluation.

Recent research showed that σ_1 R antagonists could reduce both phases of formalin-induced paw licking/biting behavior in mice.^{44,49} As a classic model of acute and chronic pain, the formalin test was performed to evaluate the antinociceptive effect of selected compounds. Intraplantar injection of formalin solution into the hind paw produces a biphasic pain response, a brief, acute phase that indicates direct effects on pain receptors (phase I), followed by a longer-lasting tonic phase that reflects inflammation (phase II). The time spent licking or biting the paw after injection was measured as an indicator of the pain response in mice. As shown in Figure 4, pretreatment with compound 137 (80 mg/kg, ip) inhibited pain responses to a similar degree as S1RA, reducing licking and biting time to 12.65 ± 5.07 s in phase I and 37.41 ± 8.89 s in phase II. S1RA at the same dose reduced licking and biting time to 10.65 ± 3.94 and 33.16 ± 7.28 s during phase I and II, respectively; the vehicle had no effect relative to treatment with formalin alone. To better characterize the antinociceptive effects of 137, a wide range of doses was tested (20–160 mg/kg). Compound 62 produced dose dependent antinociception in both phases; the ED₅₀ values were 48.36 ± 5.11 and 42.15 ± 3.96 mg/kg for phases I and II, respectively.

CCI Model. Compound 137 was evaluated in a representative and frequently used model of neuropathic pain, the CCI model in rats. Chronic constriction injury results in the

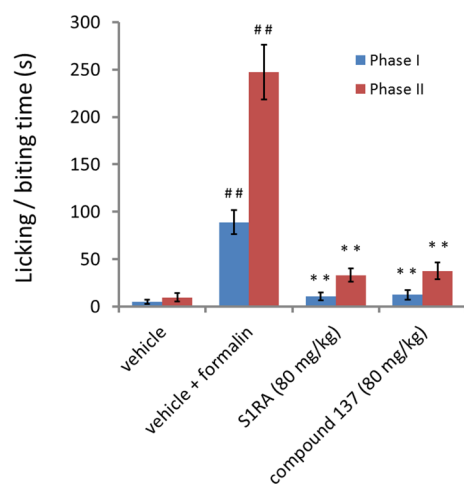
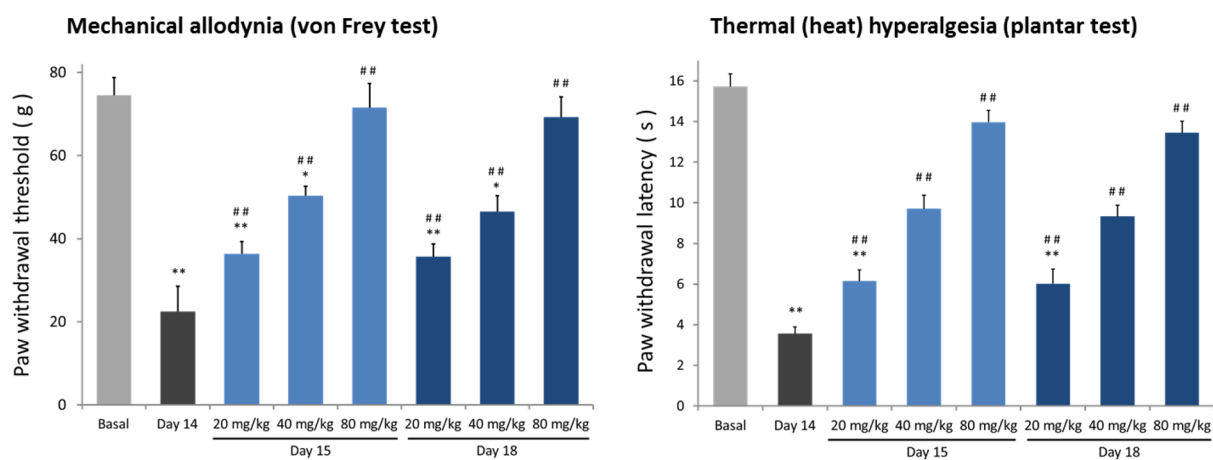


Figure 4. Antinociceptive effect of S1RA and compound 137 in phase I (0–5 min) and phase II (15–45 min) of the mice formalin test at the dose of 80 mg/kg. Each column and vertical line represents mean \pm SEM of the values obtained in at least 10 animals. Statistically significant differences: ## $p < 0.01$ vs vehicle; ** $p < 0.01$ vs vehicle + formalin (Two-Way ANOVA followed by Newman–Keuls test).

development of allodynia-like behavior, hyperalgesia, and spontaneous pain-like behavior, which are normally maximal 10–14 days after surgery.^{50,51} CCI rats exhibited signs of allodynia to mechanical stimulation and hyperalgesia to thermal stimulation, which were used as outcome measures of neuropathic pain. Mechanical allodynia was quantified by measuring the hind paw withdrawal response to von Frey hair stimulation, while thermal (heat) hyperalgesia was assessed using a plantar test by measuring hind paw withdrawal latency in response to radiant heat.

As shown in Figure 5, compound 137 dose-dependently inhibited mechanical allodynia and thermal hypersensitivity, both in single dose treatment (day 15) and repeated dose treatment (day 18), while sham operated rats did not induce significant changes in mechanical and thermal sensitivity respect to rats before surgery (basal). The ED_{50} values of single dose treatment on mechanical allodynia and thermal hypersensitivity were 58.25 ± 6.04 and 47.23 ± 3.87 mg/kg, respectively. In repeated dose treatment, the ED_{50} values of mechanical allodynia and thermal hypersensitivity were 61.82 ± 6.15 and 50.21 ± 5.07 mg/kg, respectively.

Nerve injury operation



Sham operation

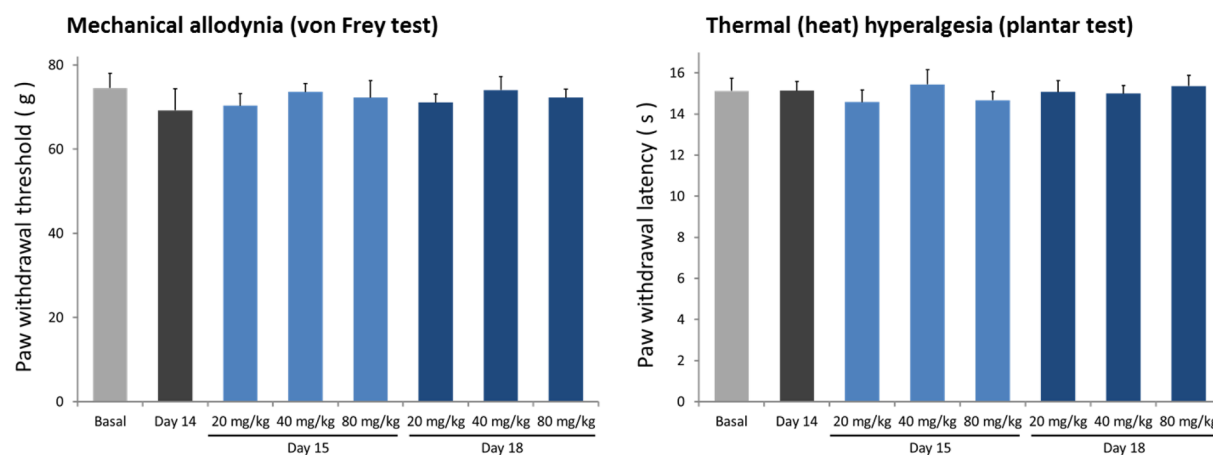


Figure 5. Antinociceptive effects of compound 137 on the expression of neuropathic pain in CCI and sham operated rats. Data obtained from 10 rats per group and expressed as mean \pm SEM pressure threshold (g) evoking paw withdrawal or latency (s) to paw withdrawal. Statistically significant differences between the rats before surgery (basal) and surgery groups: * $p < 0.05$, ** $p < 0.01$ vs basal; # $p < 0.05$; ## $p < 0.01$ vs vehicle treatment on day 14 (Two-Way ANOVA followed by Newman–Keuls test).

Motor Coordination: Rotarod Test. To investigate the possibility that the observed efficacy of compound **137** could interfere with motor coordination and thus with the response of mice in the nociceptive and neuropathic pain-related behavioral tests, motor performance was measured in the rotarod test.⁴² As shown in Figure 6, no significant effect of compound **137** at

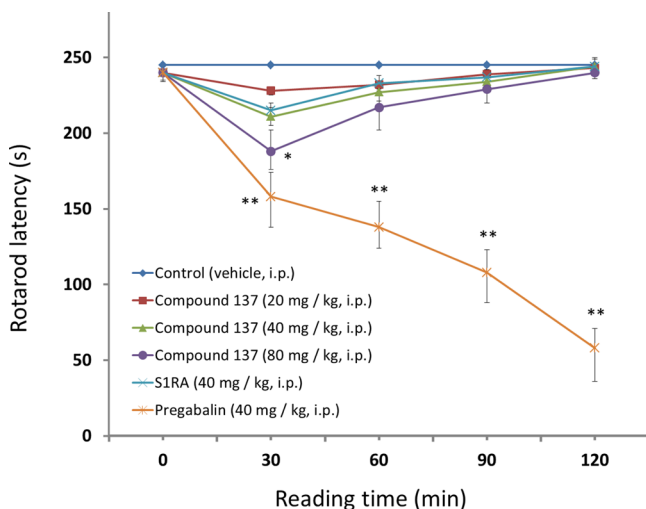


Figure 6. Dose–response effect of compound **137** and pregabalin on motor coordination (rotarod test). Data obtained from 8–10 mice per group and expressed as mean \pm SEM latency (s) to fall down from rod. Statistically significant differences: * $p < 0.05$, ** $p < 0.01$ vs vehicle (Two-Way ANOVA followed by Newman–Keuls test).

an analgesic dose was observed and no treatment-related adverse effects were found. In contrast, an analgesic dose of pregabalin induced obvious motor impairment.⁴²

Pharmacokinetic Properties of Compound 137. The evaluated pharmacokinetic properties of compound **137** included the in vitro and in vivo efficacy and the degree of safety, as characterized in rats (Table 7).

Intravenous administration of compound **137** to rats (16 mg/kg, $n = 8$) resulted in detectable plasma levels, with a half-life ($t_{1/2}$) of 10.57 h. Oral administration of compound **137** to rats (320 mg/kg, $n = 8$) resulted in a $t_{1/2}$ of 3.81 h. The area under the curve (AUC) value of compound **137** was 3295.31 ng \times h/mL after intravenous administration vs 54672.61 ng \times h/mL after oral administration. After oral administration of 320 mg/mL, compound **137** achieved a peak concentration of 17394.90 ng/mL; the T_{max} value was 0.5 h. The bioavailability of compound **137** was 75.1%. These encouraging preclinical data suggested that compound **137** possessed desirable drug-like human pharmacokinetic properties.

Selectivity Profile of Compound 137. To assess the interaction of compound **137** with other receptors or ion channels, a selectivity profile for additional receptors (such as μ -opioid, serotonergic, H_3 , cannabinoid, NMDA receptors, et. al) and ion channels (voltage-gated sodium channel Nav 1.7 and TRPV-1 protein) that implicated in pain was performed. Compound **137** showed no significant affinity (% inhibition at

1 μ M < 50%) to these targets, as shown in part S2 in Support Information.

CONCLUSIONS

A detailed structure–activity relationship investigation of pyrimidine scaffold derivatives has shown that several factors influence the binding affinity of these compounds to σ_1 and σ_2 receptors.

Pyrimidine scaffold was crucial for activity, and a basic amine was necessary matching the known σ_1 R pharmacophoric model. A straight three-carbon chain alkyl between the pyrimidine ring and the amino moiety was preferred over other linkers. The substitution on the 4-position (R_3) with a small alkyl group was preferred, and methyl was the favored substituent. The introduction of a halogen (chloro) on the 5-position (R_4) showed moderate affinities to σ_1 R and increased selectivity to σ_2 R. An aromatic group on the 2-position of the pyrimidine ring was essential for activity, and 4-chlorophenyl was favored.

From the SAR study, a series of 2-arylpyrimides were synthesized, several of which were shown to be potent and selective σ_1 R ligands. The most promising compound, **137**, showed high affinity to σ_1 receptor, low affinity to σ_2 and hERG channels, and was identified as a σ_1 R antagonist. Compound **137** exerted clear dose-dependent analgesic effects on the mice formalin-induced pain model and antinociception on both mechanical allodynia and thermal hypersensitivity in the rat CCI model. Moreover, compound **137** exhibited good safety, acceptable pharmacokinetic properties, and good selective profile to other specific targets that have been implicated in pain. Thus, compound **137** may facilitate the development of a novel class of drugs for the treatment of neuropathic pain. Further studies of compound **137** and evaluation of these series of derivatives are currently underway in our laboratory and will be reported in due course.

EXPERIMENTAL SECTION

Chemistry. Melting points were determined in open capillary tubes and are uncorrected. ^1H and ^{13}C NMR spectra were recorded on a Bruker Avance III 600 spectrometer at 600 MHz (^1H) and 150 MHz (^{13}C) using CDCl_3 as solvent. Chemical shifts are given in δ values (ppm), using tetramethylsilane (TMS) as the internal standard; coupling constants (J) are given in Hz. Signal multiplicities are characterized as s (singlet), d (doublet), t (triplet), q (quartet), m (multiplet), br (broad signal). Commercial reagents and solvents were all of analytical grade or of chemical purity (>99%). Analytical thin layer chromatography (TLC) was performed on silica gel GF254. Column chromatographic purification was carried out using silica gel. Purity analysis was carried out by LC-MS analysis using an Agilent 1200 system. The HPLC conditions are as follows: column, ZORBAX BP-C18 5.0 $\mu\text{m} \times 150 \text{ mm} \times 4.6 \text{ mm}$ I.D. (Agilent, USA); mobile phase, 30 mmol of NH_4COOH (Roe Scientific Inc., USA) aq/ acetonitrile (Merck Company, Germany), 30/70; flow rate, 1.0 mL/min; column temperature, 40 $^\circ\text{C}$. Compound purity is determined by high performance liquid chromatography (HPLC), and all final test compounds display purity higher than 95% as determined by this method.

6-Methyl-2-phenylpyrimidin-4-ol (7).⁵² To a suspension of benzimidamide hydrochloride (5, 50 mmol) and ethyl 3-oxobutanoate

Table 7. Plasma Pharmacokinetic Data Following the Administration of Compound **137** in Rats ($n = 8/\text{Group}$)

dose (mg/kg)	C_{max} (ng/kg)	T_{max} (h)	$t_{1/2}$ (h)	AUC _{0–24h} (ng \times h/mL)	AUC _{0–inf} (ng \times h/mL)	F (%)
iv 16	7261.45		10.57	3295.31	3686.17	
po 320	17394.90	0.5	3.81	54672.61	55393.45	75.1

(6, 55 mmol) in MeOH (200 mL) was added *t*-BuOK (10 mmol) portionwise with stirring at 0 °C for 30 min. The resulting mixture was heated to reflux for 4 h and then cooled down to room temperature. After that, ice–water (200 mL) was added and neutralized with citric acid. The precipitate thus formed was filtered and washed with water. The crude residue obtained was recrystallized from *i*-PrOH to give 6-methyl-2-phenylpyrimidin-4-ol, **7**, as a white solid (6.8 g, 73.0%), mp 220–222 °C. ¹H NMR (600 MHz, CDCl₃) δ 12.65 (s, 1H), 8.22–8.10 (m, 2H), 7.67–7.50 (m, 3H), 6.30 (s, 1H), 2.40 (s, 3H).

General Procedures for the Synthesis of 6-Methyl-2-phenylpyrimidinyl Derivatives (8 and 14–34). **Method A:** 4-(2-((6-Methyl-2-phenylpyrimidin-4-yl)oxy)ethyl)morpholine (**8**).⁶⁴ To a suspension of **7** (10 mmol) and 4-(2-chloroethyl) morpholine (10 mmol) in acetonitrile (100 mL), potassium carbonate (20 mmol) and a catalytic amount of potassium iodide (1% mol) were added. The resulting mixture was heated and refluxed for 6–8 h. The progress of the reaction was monitored by TLC. After filtering, the resulting filtrate was evaporated to dryness under reduced pressure. The residue was suspended in water (50 mL) and extracted with dichloromethane (3 × 25 mL). The combined organic layers were dried with anhydrous magnesium sulfate, the filtrate evaporated under reduced pressure, and the crude product was purified by means of chromatography (10% MeOH/CHCl₃) to yield 4-(2-((6-methyl-2-phenylpyrimidin-4-yl)oxy)ethyl)morpholine, **8**, as a pale-yellow oil (2.42 g, 80.9%). ¹H NMR (600 MHz, CDCl₃) δ 8.44–8.40 (m, 2H), 7.48–7.41 (m, 3H), 6.48 (s, 1H), 4.61 (t, *J* = 5.8 Hz, 2H), 3.71 (t, *J* = 4.6 Hz, 4H), 2.81 (t, *J* = 5.8 Hz, 2H), 2.57–2.51 (m, 4H), 2.48 (s, 3H). MS (ESI) *m/z* 300.3 (calcd 300.2 for C₁₇H₂₁N₃O₂ [M + H]⁺).

Method B: 4-(3-Bromopropoxy)-6-methyl-2-phenylpyrimidine (**9**). To a solution of **7** (10 mmol) and 1,3-dibromopropane (20 mmol) in acetone (100 mL), potassium carbonate (20 mmol) was added and the mixture was refluxed for 4–6 h. The progress of the reaction was monitored by TLC. After cooling to room temperature, the mixture was filtered and the solvent was evaporated under reduced pressure. The crude product was purified by means of chromatography (petroleum ether/EtOAc = 50/1) to yield 4-(3-bromopropoxy)-6-methyl-2-phenylpyrimidine, **9**, as a pale-yellow oil (1.92 g, 62.5%). ¹H NMR (600 MHz, CDCl₃) δ 8.50–8.38 (m, 2H), 7.48–7.43 (m, 3H), 6.45 (s, 1H), 4.61 (t, *J* = 6.0 Hz, 2H), 3.57 (t, *J* = 6.5 Hz, 2H), 2.49 (s, 3H), 2.38–2.32 (m, 2H). MS (ESI) *m/z* 308.3 (calcd 308.2 for C₁₄H₁₅BrN₂O [M + H]⁺).

4-(4-Bromobutoxy)-6-methyl-2-phenylpyrimidine (**10**). A pale-yellow oil (2.03 g, 63.3%). ¹H NMR (600 MHz, CDCl₃) δ 8.46–8.39 (m, 2H), 7.49–7.41 (m, 3H), 6.42 (s, 1H), 4.47 (t, *J* = 6.2 Hz, 2H), 3.46 (t, *J* = 6.6 Hz, 2H), 2.47 (s, 3H), 2.09–1.86 (m, 4H). MS (ESI) *m/z* 322.6 (calcd 322.2 for C₁₅H₁₇BrN₂O [M + H]⁺).

4-(5-Bromopentyl)oxy)-6-methyl-2-phenylpyrimidine (**11**). A pale-yellow oil (1.96 g, 58.7%). ¹H NMR (600 MHz, CDCl₃) δ 8.46–8.37 (m, 2H), 7.49–7.38 (m, 3H), 6.41 (s, 1H), 4.43 (t, *J* = 6.6 Hz, 2H), 3.39 (t, *J* = 6.8 Hz, 2H), 2.46 (s, 3H), 1.95–1.73 (m, 4H), 1.67–1.51 (m, 2H). MS (ESI) *m/z* 336.4 (calcd 336.2 for C₁₆H₁₉BrN₂O [M + H]⁺).

4-(6-Bromohexyl)oxy)-6-methyl-2-phenylpyrimidine (**12**). A pale-yellow oil (1.98 g, 56.6%). ¹H NMR (600 MHz, CDCl₃) δ 8.50–8.36 (m, 2H), 7.53–7.40 (m, 3H), 6.45 (s, 1H), 4.47 (t, *J* = 6.6 Hz, 2H), 3.42 (t, *J* = 6.8 Hz, 2H), 2.49 (s, 3H), 1.95–1.76 (m, 4H), 1.60–1.43 (m, 4H). MS (ESI) *m/z* 350.1 (calcd 350.3 for C₁₇H₂₁BrN₂O [M + H]⁺).

(E)-4-(4-Bromobut-2-en-1-yl)oxy)-6-methyl-2-phenylpyrimidine (**13**). A pale-yellow oil (2.13 g, 67.0%). ¹H NMR (600 MHz, CDCl₃) δ 8.44–8.35 (m, 2H), 7.50–7.40 (m, 3H), 6.45 (s, 1H), 6.16–5.94 (m, 2H), 4.98 (d, *J* = 5.3 Hz, 2H), 3.95 (d, *J* = 7.1 Hz, 2H), 2.47 (s, 3H). MS (ESI) *m/z* 320.3 (calcd 320.2 for C₁₅H₁₅BrN₂O [M + H]⁺).

4-(3-((6-Methyl-2-phenylpyrimidin-4-yl)oxy)propyl)morpholine (**14**). To a suspension of **9** (5 mmol) and morpholine (5.5 mmol) in acetonitrile (100 mL), cesium carbonate (10 mmol) was added, and the resulting mixture was heated and refluxed for 6–8 h. After filtering, the resulting filtrate was evaporated to dryness under reduced pressure. The residue was suspended in water (50 mL) and extracted with dichloromethane (3 × 25 mL). The combined organic layers were

dried with anhydrous magnesium sulfate, the filtrate evaporated under reduced pressure, and the crude product was purified by means of chromatography (10% MeOH/CHCl₃) to yield 4-(3-((6-methyl-2-phenylpyrimidin-4-yl)oxy)propyl)morpholine, **14**, as a pale-yellow oil (1.43 g, 91.6%). ¹H NMR (600 MHz, CDCl₃) δ 8.45–8.41 (m, 2H), 7.45–7.40 (m, 3H), 6.44 (s, 1H), 4.52 (t, *J* = 6.5 Hz, 2H), 3.71 (t, *J* = 4.6 Hz, 4H), 2.57–2.39 (m, 9H), 2.05–1.94 (m, 2H). MS (ESI) *m/z* 314.6 (calcd 314.4 for C₁₈H₂₃N₃O₂ [M + H]⁺).

4-(4-((6-Methyl-2-phenylpyrimidin-4-yl)oxy)butyl)morpholine (**15**). A pale-yellow oil (1.48 g, 90.5%). ¹H NMR (600 MHz, CDCl₃) δ 8.45–8.41 (m, 2H), 7.46–7.41 (m, 3H), 6.44 (s, 1H), 4.49 (t, *J* = 6.5 Hz, 2H), 3.70 (t, *J* = 4.6 Hz, 4H), 2.48 (s, 3H), 2.45–2.38 (m, 6H), 1.88–1.80 (m, 2H), 1.71–1.63 (m, 2H). MS (ESI) *m/z* 328.8 (calcd 328.4 for C₁₉H₂₅N₃O₂ [M + H]⁺).

4-(5-((6-Methyl-2-phenylpyrimidin-4-yl)oxy)pentyl)morpholine (**16**). A pale-yellow oil (1.50 g, 88.2%). ¹H NMR (600 MHz, CDCl₃) δ 8.46–8.38 (m, 2H), 7.46–7.40 (m, 3H), 6.45 (s, 1H), 4.48 (t, *J* = 6.6 Hz, 2H), 3.71 (t, *J* = 4.5 Hz, 4H), 2.49 (s, 3H), 2.40–2.33 (m, 6H), 1.86–1.82 (m, 2H), 1.63–1.54 (m, 2H), 1.53–1.46 (m, 2H). MS (ESI) *m/z* 342.7 (calcd 342.4 for C₂₀H₂₇N₃O₂ [M + H]⁺).

4-(6-((6-Methyl-2-phenylpyrimidin-4-yl)oxy)hexyl)morpholine (**17**). A pale-yellow oil (1.58 g, 89.4%). ¹H NMR (600 MHz, CDCl₃) δ 8.47–8.41 (m, 2H), 7.48–7.42 (m, 3H), 6.44 (s, 1H), 4.46 (t, *J* = 6.6 Hz, 2H), 3.71 (t, *J* = 4.6 Hz, 4H), 2.49 (s, 3H), 2.42–2.32 (m, 6H), 1.85–1.77 (m, 2H), 1.53–1.49 (m, 4H), 1.44–1.32 (m, 2H). MS (ESI) *m/z* 356.8 (calcd 356.5 for C₂₁H₂₉N₃O₂ [M + H]⁺).

(E)-4-(4-((6-Methyl-2-phenylpyrimidin-4-yl)oxy)but-2-en-1-yl)morpholine (**18**). A pale-yellow oil (1.41 g, 86.7%). ¹H NMR (600 MHz, CDCl₃) δ 8.46–8.39 (m, 2H), 7.49–7.42 (m, 3H), 6.46 (s, 1H), 5.97–5.83 (m, 2H), 4.98 (d, *J* = 4.2 Hz, 2H), 3.65 (t, *J* = 4.6 Hz, 4H), 3.01 (d, *J* = 4.9 Hz, 2H), 2.48 (s, 3H), 2.45–2.38 (m, 4H). MS (ESI) *m/z* 326.5 (calcd 326.4 for C₁₉H₂₃N₃O₂ [M + H]⁺).

4-Methyl-2-phenyl-6-(3-(piperidin-1-yl)propoxy)pyrimidine (**19**).⁶⁴ A yellow oil (1.42 g, 91.4%). ¹H NMR (600 MHz, CDCl₃) δ 8.48–8.37 (m, 2H), 7.47–7.41 (m, 3H), 6.44 (s, 1H), 4.50 (t, *J* = 6.5 Hz, 2H), 2.53–2.34 (m, 9H), 2.04–1.96 (m, 2H), 1.64–1.55 (m, 4H), 1.46–1.40 (m, 2H). MS (ESI) *m/z* 312.6 (calcd 312.4 for C₁₉H₂₅N₃O [M + H]⁺).

4-Methyl-6-(3-(4-methylpiperidin-1-yl)propoxy)-2-phenylpyrimidine (**20**). A yellow oil (1.40 g, 86.3%). ¹H NMR (600 MHz, CDCl₃) δ 8.50–8.36 (m, 2H), 7.54–7.41 (m, 3H), 6.43 (s, 1H), 4.50 (t, *J* = 6.5 Hz, 2H), 2.93–2.85 (m, 2H), 2.51–2.45 (m, 5H), 2.05–1.96 (m, 2H), 1.95–1.87 (m, 2H), 1.62–1.58 (m, 2H), 1.39–1.30 (m, 1H), 1.28–1.21 (m, 2H), 0.92 (d, *J* = 6.4 Hz, 3H). MS (ESI) *m/z* 326.6 (calcd 326.4 for C₂₀H₂₇N₃O [M + H]⁺).

4-(3-(3,5-Dimethylpiperidin-1-yl)propoxy)-6-methyl-2-phenylpyrimidine (**21**). A yellow oil (1.42 g, 83.5%). ¹H NMR (600 MHz, CDCl₃) δ 8.48–8.38 (m, 2H), 7.50–7.40 (m, 3H), 6.43 (s, 1H), 4.50 (t, *J* = 6.5 Hz, 2H), 2.89–2.83 (m, 2H), 2.53–2.42 (m, 5H), 2.07–1.96 (m, 2H), 1.75–1.61 (m, 4H), 1.42 (t, *J* = 10.9 Hz, 2H), 0.84 (d, *J* = 6.5 Hz, 6H). MS (ESI) *m/z* 340.8 (calcd 340.5 for C₂₁H₂₉N₃O [M + H]⁺).

4-Methyl-2-phenyl-6-(3-(2,2,6,6-tetramethylpiperidin-1-yl)propoxy)pyrimidine (**22**). A yellow oil (1.63 g, 88.6%). ¹H NMR (600 MHz, CDCl₃) δ 8.50–8.41 (m, 2H), 7.53–7.42 (m, 3H), 6.44 (s, 1H), 4.51 (t, *J* = 6.5 Hz, 2H), 2.53–2.42 (m, 5H), 2.07–1.96 (m, 2H), 1.66–1.48 (m, 4H), 1.49–1.33 (m, 2H), 0.76 (s, 12H). MS (ESI) *m/z* 368.3 (calcd 368.5 for C₂₃H₃₃N₃O [M + H]⁺).

1-(3-((6-Methyl-2-phenylpyrimidin-4-yl)oxy)propyl)piperidin-4-ol (**23**). A yellow oil (1.35 g, 82.7%). ¹H NMR (600 MHz, CDCl₃) δ 8.47–8.38 (m, 2H), 7.48–7.43 (m, 3H), 6.45 (s, 1H), 4.50 (t, *J* = 6.4 Hz, 2H), 3.66 (s, 1H), 2.84–2.74 (m, 2H), 2.67–2.43 (m, 6H), 2.18–2.07 (m, 2H), 2.03–1.96 (m, 2H), 1.92–1.83 (m, 2H), 1.63–1.54 (m, 2H). MS (ESI) *m/z* 328.8 (calcd 328.4 for C₁₉H₂₅N₃O₂ [M + H]⁺).

1-(3-((6-Methyl-2-phenylpyrimidin-4-yl)oxy)propyl)piperidin-4-one (**24**). A yellow oil (1.30 g, 80.3%). ¹H NMR (600 MHz, CDCl₃) δ 8.46–8.38 (m, 2H), 7.47–7.43 (m, 3H), 6.46 (s, 1H), 4.56 (t, *J* = 6.4 Hz, 2H), 2.76 (t, *J* = 6.1 Hz, 4H), 2.63 (t, *J* = 7.2 Hz, 2H), 2.51–2.43 (m, 7H), 2.06–1.97 (m, 2H). MS (ESI) *m/z* 326.7 (calcd 326.4 for C₁₉H₂₃N₃O₂ [M + H]⁺).

4-Methyl-2-phenyl-6-(3-(piperazin-1-yl)propoxy)pyrimidine (25). A yellow oil (1.22 g, 78.4%). ^1H NMR (600 MHz, CDCl_3) δ 8.48–8.38 (m, 2H), 7.50–7.42 (m, 3H), 6.44 (s, 1H), 4.51 (t, J = 6.5 Hz, 2H), 2.94–2.08 (m, 14H), 2.03–1.97 (m, 2H). MS (ESI) m/z 313.6 (calcd 313.4 for $\text{C}_{18}\text{H}_{24}\text{N}_4\text{O}$ [$\text{M} + \text{H}$] $^+$).

4-Methyl-6-(3-(4-methylpiperazin-1-yl)propoxy)-2-phenylpyrimidine (26). A yellow oil (1.47 g, 90.1%). ^1H NMR (600 MHz, CDCl_3) δ 8.46–8.39 (m, 2H), 7.47–7.42 (m, 3H), 6.44 (s, 1H), 4.51 (t, J = 6.5 Hz, 2H), 2.94–2.10 (m, 16H), 2.03–1.97 (m, 2H). MS (ESI) m/z 327.6 (calcd 327.4 for $\text{C}_{19}\text{H}_{26}\text{N}_4\text{O}$ [$\text{M} + \text{H}$] $^+$).

4-(3-(4-Ethylpiperazin-1-yl)propoxy)-6-methyl-2-phenylpyrimidine (27). A yellow oil (1.48 g, 87.1%). ^1H NMR (600 MHz, CDCl_3) δ 8.48–8.40 (m, 2H), 7.46–7.41 (m, 3H), 6.44 (s, 1H), 4.51 (t, J = 6.5 Hz, 2H), 2.95–2.17 (m, 15H), 2.02–1.96 (m, 2H), 1.08 (t, J = 7.2 Hz, 3H). MS (ESI) m/z 341.4 (calcd 341.5 for $\text{C}_{20}\text{H}_{28}\text{N}_4\text{O}$ [$\text{M} + \text{H}$] $^+$).

1-Methyl-4-(3-((6-methyl-2-phenylpyrimidin-4-yl)oxy)propyl)-1,4-diazepane (28). A yellow oil (1.49 g, 87.6%). ^1H NMR (600 MHz, CDCl_3) δ 8.46–8.40 (m, 2H), 7.48–7.43 (m, 3H), 6.45 (s, 1H), 4.52 (t, J = 6.5 Hz, 2H), 2.85–2.28 (m, 15H), 2.02–1.94 (m, 2H), 1.86–1.80 (m, 2H). MS (ESI) m/z 341.7 (calcd 341.5 for $\text{C}_{20}\text{H}_{28}\text{N}_4\text{O}$ [$\text{M} + \text{H}$] $^+$).

4-(3-(4-Boc-piperazin-1-yl)propoxy)-6-methyl-2-phenylpyrimidine (29). A yellow oil (1.75 g, 85.2%). ^1H NMR (600 MHz, CDCl_3) δ 8.48–8.38 (m, 2H), 7.48–7.42 (m, 3H), 6.44 (s, 1H), 4.52 (t, J = 6.4 Hz, 2H), 3.44 (s, 4H), 2.57–2.46 (m, 5H), 2.46–2.24 (m, 4H), 2.02–1.97 (m, 2H), 1.46 (s, 9H). MS (ESI) m/z 413.7 (calcd 413.5 for $\text{C}_{23}\text{H}_{32}\text{N}_4\text{O}_3$ [$\text{M} + \text{H}$] $^+$).

4-Methyl-2-phenyl-6-(3-(4-phenylpiperazin-1-yl)propoxy)pyrimidine (30). A yellow oil (1.71 g, 88.1%). ^1H NMR (600 MHz, CDCl_3) δ 8.46–8.41 (m, 2H), 7.48–7.44 (m, 3H), 7.29–7.24 (m, 2H), 6.96–6.91 (m, 2H), 6.88–6.82 (m, 1H), 6.46 (s, 1H), 4.56 (t, J = 6.4 Hz, 2H), 3.28–3.15 (m, 4H), 2.68–2.62 (m, 4H), 2.61–2.56 (m, 2H), 2.49 (s, 3H), 2.08–2.02 (m, 2H). MS (ESI) m/z 389.2 (calcd 389.5 for $\text{C}_{24}\text{H}_{28}\text{N}_4\text{O}$ [$\text{M} + \text{H}$] $^+$).

4-Methyl-2-phenyl-6-(3-(pyrrolidin-1-yl)propoxy)pyrimidine (31). A pale-red oil (1.36 g, 91.5%). ^1H NMR (600 MHz, CDCl_3) δ 8.44–8.40 (m, 2H), 7.46–7.43 (m, 3H), 6.45 (s, 1H), 4.53 (t, J = 6.5 Hz, 2H), 2.66–2.60 (m, 2H), 2.57–2.51 (m, 4H), 2.48 (s, 3H), 2.07–2.01 (m, 2H), 1.82–1.76 (m, 4H). MS (ESI) m/z 298.8 (calcd 289.4 for $\text{C}_{18}\text{H}_{23}\text{N}_3\text{O}$ [$\text{M} + \text{H}$] $^+$).

***N,N*-Dimethyl-3-((6-methyl-2-phenylpyrimidin-4-yl)oxy)propan-1-amine (32).** A yellow oil (1.05 g, 77.4%). ^1H NMR (600 MHz, CDCl_3) δ 8.46–8.41 (m, 2H), 7.44–7.41 (m, 3H), 6.41 (s, 1H), 4.48 (t, J = 6.5 Hz, 2H), 2.46–2.40 (m, 5H), 2.23 (s, 6H), 1.99–1.91 (m, 2H). MS (ESI) m/z 272.6 (calcd 272.4 for $\text{C}_{16}\text{H}_{21}\text{N}_3\text{O}$ [$\text{M} + \text{H}$] $^+$).

***N,N*-Diethyl-3-((6-methyl-2-phenylpyrimidin-4-yl)oxy)propan-1-amine (33).** A yellow oil (1.13 g, 76.1%). ^1H NMR (600 MHz, CDCl_3) δ 8.47–8.41 (m, 2H), 7.50–7.43 (m, 3H), 6.45 (s, 1H), 4.51 (t, J = 6.5 Hz, 2H), 2.64–2.59 (m, 2H), 2.58–2.52 (m, 4H), 2.48 (s, 3H), 2.00–1.92 (m, 2H), 1.03 (t, J = 7.2 Hz, 6H). MS (ESI) m/z 300.2 (calcd 300.4 for $\text{C}_{18}\text{H}_{25}\text{N}_3\text{O}$ [$\text{M} + \text{H}$] $^+$).

3-((6-Methyl-2-phenylpyrimidin-4-yl)oxy)-*N,N*-dipropylpropan-1-amine (34). A yellow oil (1.31 g, 80.2%). ^1H NMR (600 MHz, CDCl_3) δ 8.48–8.38 (m, 2H), 7.48–7.43 (m, 3H), 6.45 (s, 1H), 4.51 (t, J = 6.5 Hz, 2H), 2.63–2.57 (m, 2H), 2.49 (s, 3H), 2.42–2.36 (m, 4H), 1.99–1.91 (m, 2H), 1.51–1.41 (m, 4H), 0.87 (t, J = 7.4 Hz, 6H). MS (ESI) m/z 328.5 (calcd 328.5 for $\text{C}_{20}\text{H}_{29}\text{N}_3\text{O}$ [$\text{M} + \text{H}$] $^+$).

4-(2-(2-Bromoethoxy)ethoxy)-6-methyl-2-phenylpyrimidine (35). To a solution of 7 (10 mmol) and 1-bromo-2-(2-bromoethoxy)ethane (20 mmol) in acetone (100 mL), potassium carbonate (20 mmol), and a catalytic amount of potassium iodide (1% mol) were added. The mixture was refluxed for 4–6 h, and the progress was monitored by TLC. After cooling to room temperature, the mixture was filtered and the solvent was evaporated under reduced pressure. The crude product was purified by means of chromatography (petroleum ether/EtOAc = 100/1 to 50/1) to yield 4-(2-(2-bromoethoxy)ethoxy)-6-methyl-2-phenylpyrimidine, 35, as a pale-yellow oil (1.85 g, 54.8%). ^1H NMR (600 MHz, CDCl_3) δ 8.47–8.36 (m, 2H), 7.50–7.40 (m, 3H), 6.50 (s, 1H), 4.64 (t, J = 6.4 Hz, 2H), 3.88 (t, J = 6.3 Hz, 2H), 3.84 (t, J = 6.3 Hz, 2H), 3.47 (t, J = 6.3 Hz, 2H), 2.48 (s, 3H). MS (ESI) m/z 338.1 (calcd 338.2 for $\text{C}_{15}\text{H}_{17}\text{BrN}_2\text{O}_2$ [$\text{M} + \text{H}$] $^+$).

4-(2-(2-((6-Methyl-2-phenylpyrimidin-4-yl)oxy)ethoxy)ethyl)morpholine (36). To a suspension of 35 (5 mmol) and morpholine (5.5 mmol) in acetonitrile (100 mL), cesium carbonate (10 mmol) was added and the resulting mixture was heated and refluxed for 6–8 h. After filtering, the resulting filtrate was evaporated to dryness under reduced pressure. The residue was suspended in water (50 mL) and extracted with dichloromethane (3 \times 25 mL). The combined organic layers were dried with anhydrous magnesium sulfate, the filtrate evaporated under reduced pressure, and the crude product purified by means of chromatography (10% MeOH/ CHCl_3) to yield 4-(2-(2-((6-methyl-2-phenylpyrimidin-4-yl)oxy)ethoxy)ethyl)morpholine, 36, as a pale-yellow oil (1.49 g, 86.7%). ^1H NMR (600 MHz, CDCl_3) δ 8.47–8.38 (m, 2H), 7.50–7.40 (m, 3H), 6.50 (s, 1H), 4.65 (t, J = 6.6 Hz, 2H), 3.88–3.79 (m, 2H), 3.72–3.66 (m, 6H), 2.62–2.56 (m, 2H), 2.49–2.39 (m, 7H). MS (ESI) m/z 344.7 (calcd 344.4 for $\text{C}_{19}\text{H}_{25}\text{N}_3\text{O}_3$ [$\text{M} + \text{H}$] $^+$).

4-Methyl-6-(oxiran-2-ylmethoxy)-2-phenylpyrimidine (37). To a suspension of 7 (10 mmol) and 2-(chloromethyl)oxirane (11 mmol) in acetonitrile (100 mL), potassium carbonate (20 mmol) and a catalytic amount of potassium iodide (1% mol) were added. The resulting mixture was heated and refluxed for 4–6 h, and the progress of the reaction was monitored by TLC. After cooling to room temperature, the mixture was filtered and the solvent was evaporated under reduced pressure. The crude product was purified by means of chromatography (petroleum ether/EtOAc = 40/1) to yield 4-methyl-6-(oxiran-2-ylmethoxy)-2-phenylpyrimidine, 37, as a pale-yellow oil (1.77 g, 71.1%). ^1H NMR (600 MHz, CDCl_3) δ 8.44–8.24 (m, 2H), 7.43–7.33 (m, 3H), 6.44 (s, 1H), 4.82–4.14 (m, 2H), 3.40–3.22 (m, 1H), 2.91–2.60 (m, 2H), 2.42 (s, 3H). MS (ESI) m/z 243.5 (calcd 243.3 for $\text{C}_{14}\text{H}_{14}\text{N}_2\text{O}_2$ [$\text{M} + \text{H}$] $^+$).

1-((6-Methyl-2-phenylpyrimidin-4-yl)oxy)-3-morpholinopropan-2-ol (38). A mixture of 37 and (5 mmol) and morpholine (5.5 mmol) in MeOH was stirred and heated to reflux for 6–8 h. The solvent was evaporated under reduced pressure, and the crude product was purified by means of chromatography (petroleum ether/EtOAc = 10/1 to EtOAc) to yield 1-((6-methyl-2-phenylpyrimidin-4-yl)oxy)-3-morpholinopropan-2-ol, 38, as a yellow oil (0.83 g, 50.6%). ^1H NMR (600 MHz, CDCl_3) δ 8.44–8.35 (m, 2H), 7.51–7.46 (m, 3H), 6.53 (s, 1H), 4.35–4.26 (m, 2H), 4.12–4.08 (m, 2H), 3.85–3.64 (m, 6H), 2.57–2.54 (m, 4H), 2.51 (s, 3H). MS (ESI) m/z 330.4 (calcd 330.4 for $\text{C}_{18}\text{H}_{23}\text{N}_3\text{O}_3$ [$\text{M} + \text{H}$] $^+$).

General Procedures for the Synthesis of 2-Phenylpyrimidinyl Derivatives (49–58).^{53–59}

6-Ethyl-2-phenylpyrimidin-4-ol (49). To a suspension of benzimidamide hydrochloride (5, 50 mmol) and ethyl 3-oxopentanoate (39, 55 mmol) in MeOH (200 mL) was added *t*-BuOK (10 mmol) portionwise, with stirring, at 0 $^\circ\text{C}$ for 30 min. The resulting mixture was heated to reflux for 4 h and then cooled down to room temperature. After that, ice–water (200 mL) was added and neutralized with citric acid. The precipitate thus formed was filtered and washed with water. The crude residue obtained was recrystallized from *i*-PrOH to give 6-ethyl-2-phenylpyrimidin-4-ol, 49, as a white solid (7.60 g, 75.9%), mp 166–168 $^\circ\text{C}$. ^1H NMR (600 MHz, CDCl_3) δ 13.15 (s, 1H), 8.33–8.12 (m, 2H), 7.63–7.45 (m, 3H), 6.31 (s, 1H), 2.67 (q, J = 7.5 Hz, 2H), 1.30 (t, J = 7.5 Hz, 3H).

2-Phenyl-6-propylpyrimidin-4-ol (50). A white solid (8.20 g, 76.7%), mp 145–147 $^\circ\text{C}$. ^1H NMR (600 MHz, CDCl_3) δ 12.84 (s, 1H), 8.26–8.15 (m, 2H), 7.66–7.48 (m, 3H), 6.29 (s, 1H), 2.61 (t, J = 7.6 Hz, 2H), 1.86–1.73 (m, 2H), 1.01 (t, J = 7.4 Hz, 3H).

6-Isopropyl-2-phenylpyrimidin-4-ol (51). A white solid (8.37 g, 78.2%), mp 133–136 $^\circ\text{C}$. ^1H NMR (600 MHz, CDCl_3) δ 13.16 (s, 1H), 8.36–8.16 (m, 2H), 7.67–7.43 (m, 3H), 6.31 (s, 1H), 3.00–2.71 (m, 1H), 1.30 (d, J = 6.9 Hz, 6H).

6-Methoxy-2-phenylpyrimidin-4-ol (52). A white solid (7.31 g, 72.3%), mp 112–115 $^\circ\text{C}$. ^1H NMR (600 MHz, CDCl_3) δ 13.24 (s, 1H), 8.38–8.12 (m, 2H), 7.67–7.49 (m, 3H), 6.59 (s, 1H), 3.52 (s, 3H).

2-Phenyl-6-(trifluoromethyl)pyrimidin-4-ol (53). A white solid (9.46 g, 78.8%), mp 107–110 $^\circ\text{C}$. ^1H NMR (600 MHz, CDCl_3) δ 12.78 (s, 1H), 8.45–8.13 (m, 2H), 7.89–7.47 (m, 3H), 6.84 (s, 1H).

6-Cyclopropyl-2-phenylpyrimidin-4-ol (54). A white solid (8.41 g, 79.2%), mp 181–183 °C. ^1H NMR (600 MHz, CDCl_3) δ 12.93 (s, 1H), 8.39–8.02 (m, 2H), 7.65–7.42 (m, 3H), 6.33 (s, 1H), 2.00–1.74 (m, 1H), 1.35–1.13 (m, 2H), 1.08–0.86 (m, 2H).

2,6-Diphenylpyrimidin-4-ol (55). A white solid (9.98 g, 80.4%), mp 285–288 °C. ^1H NMR (600 MHz, CDCl_3) δ 11.50 (s, 1H), 8.28–8.20 (m, 2H), 8.17–8.09 (m, 2H), 7.68–7.45 (m, 6H), 6.89 (s, 1H).

5,6-Dimethyl-2-phenylpyrimidin-4-ol (56). A white solid (7.44 g, 74.3%), mp 157–160 °C. ^1H NMR (600 MHz, CDCl_3) δ 13.36 (s, 1H), 8.40–8.14 (m, 2H), 7.65–7.40 (m, 3H), 2.41 (s, 3H), 2.13 (s, 3H).

5-Fluoro-6-methyl-2-phenylpyrimidin-4-ol (57). A white solid (7.18 g, 70.3%), mp 148–151 °C. ^1H NMR (600 MHz, CDCl_3) δ 13.13 (s, 1H), 8.34–7.97 (m, 2H), 7.67–7.44 (m, 3H), 2.43 (s, 3H).

5-Chloro-6-methyl-2-phenylpyrimidin-4-ol (58). A white solid (7.88 g, 71.4%), mp 166–169 °C. ^1H NMR (600 MHz, CDCl_3) δ 12.86 (s, 1H), 8.27–7.95 (m, 2H), 7.70–7.37 (m, 2H), 2.55 (s, 3H).

General Procedures for the Synthesis of 2-Phenyl-6-(3-(piperidin-1-yl)propoxy)pyrimidine Derivatives (59–78). 4-(3-Bromopropoxy)-6-ethyl-2-phenylpyrimidine (59). To a solution of 49 (10 mmol) and 1,3-dibromopropane (20 mmol) in acetone (100 mL), potassium carbonate (20 mmol) was added and the mixture was refluxed for 4–6 h. The progress of the reaction was monitored by TLC. After cooling to room temperature, the mixture was filtered and the solvent was evaporated under reduced pressure. The crude product was purified by means of chromatography (petroleum ether/EtOAc = 50/1) to yield 4-(3-bromopropoxy)-6-ethyl-2-phenylpyrimidine, 59, as a pale-yellow oil (1.95 g, 60.8%). ^1H NMR (600 MHz, CDCl_3) δ 8.49–8.40 (m, 2H), 7.49–7.43 (m, 3H), 6.46 (s, 1H), 4.62 (t, J = 6.0 Hz, 2H), 3.58 (t, J = 6.5 Hz, 2H), 2.77 (q, J = 7.6 Hz, 2H), 2.42–2.31 (m, 2H), 1.33 (t, J = 7.6 Hz, 3H). MS (ESI) m/z 322.4 (calcd 322.2 for $\text{C}_{15}\text{H}_{17}\text{BrN}_2\text{O}$ [$\text{M} + \text{H}$] $^+$).

4-(3-Bromopropoxy)-2-phenyl-6-propylpyrimidine (60). A pale-yellow oil (2.08 g, 62.2%). ^1H NMR (600 MHz, CDCl_3) δ 8.49–8.40 (m, 2H), 7.49–7.43 (m, 3H), 6.46 (s, 1H), 4.62 (t, J = 6.0 Hz, 2H), 3.58 (t, J = 6.5 Hz, 2H), 2.77 (q, J = 7.6 Hz, 2H), 2.42–2.31 (m, 2H), 1.33 (t, J = 7.6 Hz, 3H). MS (ESI) m/z 336.4 (calcd 336.2 for $\text{C}_{16}\text{H}_{19}\text{BrN}_2\text{O}$ [$\text{M} + \text{H}$] $^+$).

4-(3-Bromopropoxy)-6-isopropyl-2-phenylpyrimidine (61). A pale-yellow oil (2.03 g, 60.7%). ^1H NMR (600 MHz, CDCl_3) δ 8.53–8.36 (m, 2H), 7.49–7.42 (m, 3H), 6.46 (s, 1H), 4.61 (t, J = 6.0 Hz, 2H), 3.57 (t, J = 6.5 Hz, 2H), 3.50 (s, 3H), 2.39–2.31 (m, 2H), 1.32 (d, J = 6.9 Hz, 6H). MS (ESI) m/z 336.7 (calcd 336.2 for $\text{C}_{16}\text{H}_{19}\text{BrN}_2\text{O}$ [$\text{M} + \text{H}$] $^+$).

4-(3-Bromopropoxy)-6-methoxy-2-phenylpyrimidine (62). A pale-yellow oil (1.88 g, 58.2%). ^1H NMR (600 MHz, CDCl_3) δ 8.47–8.36 (m, 2H), 7.48–7.42 (m, 3H), 6.75 (s, 1H), 4.62 (t, J = 6.0 Hz, 2H), 3.57 (t, J = 6.5 Hz, 2H), 3.50 (s, 3H), 2.39–2.31 (m, 2H). MS (ESI) m/z 324.5 (calcd 324.2 for $\text{C}_{14}\text{H}_{15}\text{BrN}_2\text{O}_2$ [$\text{M} + \text{H}$] $^+$).

4-(3-Bromopropoxy)-2-phenyl-6-(trifluoromethyl)pyrimidine (63). A pale-yellow oil (2.22 g, 61.4%). ^1H NMR (600 MHz, CDCl_3) δ 8.50–8.40 (m, 2H), 7.55–7.38 (m, 3H), 6.88 (s, 1H), 4.66 (t, J = 6.0 Hz, 2H), 3.56 (t, J = 6.4 Hz, 2H), 2.42–2.31 (m, 2H). MS (ESI) m/z 362.6 (calcd 362.2 for $\text{C}_{14}\text{H}_{12}\text{BrF}_3\text{N}_2\text{O}$ [$\text{M} + \text{H}$] $^+$).

4-(3-Bromopropoxy)-6-cyclopropyl-2-phenylpyrimidine (64). A pale-yellow oil (2.13 g, 63.8%). ^1H NMR (600 MHz, CDCl_3) δ 8.47–8.31 (m, 2H), 7.48–7.41 (m, 3H), 6.46 (s, 1H), 4.61 (t, J = 6.0 Hz, 2H), 3.59 (t, J = 6.5 Hz, 2H), 2.43–2.30 (m, 2H), 2.02–1.91 (m, 1H), 1.24–1.21 (m, 2H), 1.05–1.01 (m, 2H). MS (ESI) m/z 334.1 (calcd 334.2 for $\text{C}_{16}\text{H}_{17}\text{BrN}_2\text{O}$ [$\text{M} + \text{H}$] $^+$).

4-(3-Bromopropoxy)-2,6-diphenylpyrimidine (65). A pale-yellow oil (2.44 g, 66.1%). ^1H NMR (600 MHz, CDCl_3) δ 8.64–8.51 (m, 2H), 8.22–8.14 (m, 2H), 7.53–7.47 (m, 6H), 7.02 (s, 1H), 4.70 (t, J = 6.0 Hz, 2H), 3.62 (t, J = 6.5 Hz, 2H), 2.47–2.37 (m, 2H). MS (ESI) m/z 370.2 (calcd 370.3 for $\text{C}_{19}\text{H}_{17}\text{BrN}_2\text{O}$ [$\text{M} + \text{H}$] $^+$).

4-(3-Bromopropoxy)-5,6-dimethyl-2-phenylpyrimidine (66). A pale-yellow oil (1.90 g, 59.3%). ^1H NMR (600 MHz, CDCl_3) δ 8.44–8.34 (m, 2H), 7.52–7.36 (m, 3H), 4.62 (t, J = 6.0 Hz, 2H), 3.59 (t, J = 6.6 Hz, 2H), 2.49 (s, 3H), 2.43–2.34 (m, 2H), 2.13 (s, 3H). MS (ESI) m/z 322.6 (calcd 322.2 for $\text{C}_{15}\text{H}_{17}\text{BrN}_2\text{O}$ [$\text{M} + \text{H}$] $^+$).

4-(3-Bromopropoxy)-5-fluoro-6-methyl-2-phenylpyrimidine (67). A pale-yellow oil (1.95 g, 60.1%). ^1H NMR (600 MHz, CDCl_3) δ 8.42–8.26 (m, 2H), 7.51–7.40 (m, 3H), 4.70 (t, J = 6.0 Hz, 2H), 3.61 (t, J = 6.4 Hz, 2H), 2.52 (s, 3H), 2.45–2.36 (m, 2H). MS (ESI) m/z 326.1 (calcd 326.2 for $\text{C}_{14}\text{H}_{14}\text{BrFN}_2\text{O}$ [$\text{M} + \text{H}$] $^+$).

4-(3-Bromopropoxy)-5-chloro-6-methyl-2-phenylpyrimidine (68). A pale-yellow oil (2.12 g, 62.2%). ^1H NMR (600 MHz, CDCl_3) δ 8.46–8.33 (m, 2H), 7.51–7.41 (m, 3H), 4.69 (t, J = 6.0 Hz, 2H), 3.62 (t, J = 6.5 Hz, 2H), 2.62 (s, 3H), 2.47–2.35 (m, 2H). MS (ESI) m/z 342.8 (calcd 342.6 for $\text{C}_{14}\text{H}_{14}\text{BrClN}_2\text{O}$ [$\text{M} + \text{H}$] $^+$).

4-Ethyl-2-phenyl-6-(3-(piperidin-1-yl)propoxy)pyrimidine (69). A mixture of 59 (5 mmol) and piperidine (5.5 mmol) in acetonitrile (100 mL) and cesium carbonate (10 mmol) was heated and refluxed for 6–8 h. After filtering, the resulting filtrate was evaporated to dryness under reduced pressure. The residue was suspended in water (50 mL) and extracted with dichloromethane (3 \times 25 mL). The combined organic layers were dried with anhydrous magnesium sulfate, the filtrate evaporated under reduced pressure, and the crude product purified by means of chromatography (10% MeOH/ CHCl_3) to yield 4-ethyl-2-phenyl-6-(3-(piperidin-1-yl)propoxy)pyrimidine, 69, as a yellow oil (1.41 g, 86.4%). ^1H NMR (600 MHz, CDCl_3) δ 8.49–8.41 (m, 2H), 7.49–7.43 (m, 3H), 6.45 (s, 1H), 4.52 (t, J = 6.5 Hz, 2H), 2.77 (q, J = 7.6 Hz, 2H), 2.52–2.33 (m, 6H), 2.06–1.97 (m, 2H), 1.64–1.57 (m, 4H), 1.50–1.38 (m, 2H), 1.33 (t, J = 7.6 Hz, 3H). MS (ESI) m/z 326.5 (calcd 326.4 for $\text{C}_{20}\text{H}_{27}\text{N}_3\text{O}$ [$\text{M} + \text{H}$] $^+$).

2-Phenyl-4-(3-(piperidin-1-yl)propoxy)-6-propylpyrimidine (70). A yellow oil (1.50 g, 88.3%). ^1H NMR (600 MHz, CDCl_3) δ 8.51–8.44 (m, 2H), 7.50–7.42 (m, 3H), 6.45 (s, 1H), 4.53 (t, J = 6.5 Hz, 2H), 2.75–2.69 (m, 2H), 2.55–2.29 (m, 6H), 2.08–1.99 (m, 2H), 1.87–1.77 (m, 2H), 1.65–1.58 (m, 4H), 1.51–1.40 (m, 2H), 1.01 (t, J = 7.4 Hz, 3H). MS (ESI) m/z 340.8 (calcd 340.5 for $\text{C}_{21}\text{H}_{29}\text{N}_3\text{O}$ [$\text{M} + \text{H}$] $^+$).

4-Isopropyl-2-phenyl-6-(3-(piperidin-1-yl)propoxy)pyrimidine (71). A yellow oil (1.51 g, 89.2%). ^1H NMR (600 MHz, CDCl_3) δ 8.52–8.46 (m, 2H), 7.50–7.44 (m, 3H), 6.48 (s, 1H), 4.54 (t, J = 6.5 Hz, 2H), 3.00 (dt, J = 13.8, 6.9 Hz, 1H), 2.54–2.36 (m, 6H), 2.09–2.01 (m, 2H), 1.66–1.59 (m, 4H), 1.51–1.42 (m, 2H), 1.35 (d, J = 6.9 Hz, 6H). MS (ESI) m/z 340.2 (calcd 340.5 for $\text{C}_{21}\text{H}_{29}\text{N}_3\text{O}$ [$\text{M} + \text{H}$] $^+$).

4-Methoxy-2-phenyl-6-(3-(piperidin-1-yl)propoxy)pyrimidine (72). A yellow oil (1.37 g, 84.1%). ^1H NMR (600 MHz, CDCl_3) δ 8.45–8.39 (m, 2H), 7.46–7.40 (m, 3H), 6.74 (s, 1H), 4.52 (t, J = 6.5 Hz, 2H), 3.50 (s, 3H), 2.51–2.38 (m, 6H), 2.07–1.97 (m, 2H), 1.65–1.55 (m, 4H), 1.45–1.38 (m, 2H). MS (ESI) m/z 328.5 (calcd 328.4 for $\text{C}_{19}\text{H}_{25}\text{N}_3\text{O}_2$ [$\text{M} + \text{H}$] $^+$).

2-Phenyl-4-(3-(piperidin-1-yl)propoxy)-6-(trifluoromethyl)pyrimidine (73). A yellow oil (1.57 g, 86.2%). ^1H NMR (600 MHz, CDCl_3) δ 8.52–8.42 (m, 2H), 7.52–7.44 (m, 3H), 6.90 (s, 1H), 4.59 (t, J = 6.5 Hz, 2H), 2.52–2.36 (m, 6H), 2.09–2.00 (m, 2H), 1.66–1.55 (m, 4H), 1.48–1.42 (m, 2H). MS (ESI) m/z 366.4 (calcd 366.4 for $\text{C}_{19}\text{H}_{22}\text{F}_3\text{N}_3\text{O}$ [$\text{M} + \text{H}$] $^+$).

4-Cyclopropyl-2-phenyl-6-(3-(piperidin-1-yl)propoxy)pyrimidine (74). A yellow oil (1.53 g, 90.5%). ^1H NMR (600 MHz, CDCl_3) δ 8.45–8.37 (m, 2H), 7.61–7.48 (m, 3H), 6.39 (s, 1H), 4.51 (t, J = 6.5 Hz, 2H), 2.53–2.34 (m, 6H), 2.04–1.84 (m, 3H), 1.66–1.53 (m, 4H), 1.46–1.41 (m, 2H), 1.29–1.14 (m, 2H), 1.08–0.95 (m, 2H). MS (ESI) m/z 338.2 (calcd 338.5 for $\text{C}_{21}\text{H}_{27}\text{N}_3\text{O}$ [$\text{M} + \text{H}$] $^+$).

2,4-Diphenyl-6-(3-(piperidin-1-yl)propoxy)pyrimidine (75). A yellow oil (1.71 g, 91.4%). ^1H NMR (600 MHz, CDCl_3) δ 8.62–8.54 (m, 2H), 8.22–8.15 (m, 2H), 7.54–7.46 (m, 6H), 7.02 (s, 1H), 4.58 (t, J = 6.5 Hz, 2H), 2.56–2.37 (m, 6H), 2.06–1.96 (m, 2H), 1.66–1.58 (m, 4H), 1.45–1.38 (m, 2H). MS (ESI) m/z 374.8 (calcd 374.5 for $\text{C}_{24}\text{H}_{27}\text{N}_3\text{O}$ [$\text{M} + \text{H}$] $^+$).

4,5-Dimethyl-2-phenyl-6-(3-(piperidin-1-yl)propoxy)pyrimidine (76). A yellow oil (1.42 g, 87.1%). ^1H NMR (600 MHz, CDCl_3) δ 8.44–8.36 (m, 2H), 7.48–7.37 (m, 3H), 4.51 (t, J = 6.4 Hz, 2H), 2.56–2.30 (m, 9H), 2.12 (s, 3H), 2.06–1.97 (m, 2H), 1.64–1.55 (m, 4H), 1.47–1.41 (m, 2H). MS (ESI) m/z 326.6 (calcd 326.4 for $\text{C}_{20}\text{H}_{27}\text{N}_3\text{O}$ [$\text{M} + \text{H}$] $^+$).

5-Fluoro-4-methyl-2-phenyl-6-(3-(piperidin-1-yl)propoxy)pyrimidine (77). A yellow oil (1.36 g, 82.6%). ^1H NMR (600 MHz, CDCl_3) δ 8.38–8.28 (m, 2H), 7.48–7.39 (m, 3H), 4.58 (t, J = 6.6 Hz, 2H), 2.62–2.26 (m, 9H), 2.12–1.98 (m, 2H), 1.66–1.52 (m, 4H), 1.46–1.41 (m, 2H). MS (ESI) m/z 330.2 (calcd 330.4 for $\text{C}_{19}\text{H}_{24}\text{FN}_3\text{O}$ $[\text{M} + \text{H}]^+$).

5-Chloro-4-methyl-2-phenyl-6-(3-(piperidin-1-yl)propoxy)pyrimidine (78). A yellow oil (1.41 g, 81.5%). ^1H NMR (600 MHz, CDCl_3) δ 8.44–8.33 (m, 2H), 7.49–7.40 (m, 3H), 4.61 (t, J = 6.5 Hz, 2H), 2.72–2.65 (m, 2H), 2.64–2.51 (m, 7H), 2.14–2.06 (m, 2H), 1.85–1.75 (m, 4H), 1.44–1.39 (m, 2H). MS (ESI) m/z 346.9 (calcd 346.9 for $\text{C}_{19}\text{H}_{24}\text{ClN}_3\text{O}$ $[\text{M} + \text{H}]^+$).

General Procedures for the Synthesis of 2-Phenyl-6-(3-(pyrrolidin-1-yl)propoxy)pyrimidine Derivatives (79–88). **4-Ethyl-2-phenyl-6-(3-(pyrrolidin-1-yl)propoxy)pyrimidine (79).** A mixture of **59** (5 mmol) and pyrrolidine (5.5 mmol) in acetonitrile (100 mL) and cesium carbonate (10 mmol) was heated and refluxed for 6–8 h. After filtering, the resulting filtrate was evaporated to dryness under reduced pressure. The residue was suspended in water (50 mL) and extracted with dichloromethane (3×25 mL). The combined organic layers were dried with anhydrous magnesium sulfate, the filtrate evaporated under reduced pressure, and the crude product purified by means of chromatography (10% MeOH/ CHCl_3) to yield 4-ethyl-2-phenyl-6-(3-(pyrrolidin-1-yl)propoxy)pyrimidine, **79**, as a pale-red oil (1.37 g, 88.2%). ^1H NMR (600 MHz, CDCl_3) δ 8.48–8.41 (m, 2H), 7.48–7.43 (m, 3H), 6.46 (s, 1H), 4.54 (t, J = 6.5 Hz, 2H), 2.77 (q, J = 7.6 Hz, 2H), 2.67–2.62 (m, 2H), 2.58–2.50 (m, 4H), 2.09–2.01 (m, 2H), 1.84–1.75 (m, 4H), 1.33 (t, J = 7.6 Hz, 3H). MS (ESI) m/z 312.8 (calcd 312.4 for $\text{C}_{19}\text{H}_{25}\text{N}_3\text{O}$ $[\text{M} + \text{H}]^+$).

2-Phenyl-4-(3-(pyrrolidin-1-yl)propoxy)-6-propylpyrimidine (80). A pale-red oil (1.40 g, 86.2%). ^1H NMR (600 MHz, CDCl_3) δ 8.47–8.40 (m, 2H), 7.47–7.43 (m, 3H), 6.44 (s, 1H), 4.53 (t, J = 6.5 Hz, 2H), 2.73–2.68 (m, 2H), 2.67–2.61 (m, 2H), 2.58–2.51 (m, 4H), 2.08–2.02 (m, 2H), 1.83–1.77 (m, 6H), 1.00 (t, J = 7.4 Hz, 3H). MS (ESI) m/z 326.6 (calcd 326.4 for $\text{C}_{20}\text{H}_{27}\text{N}_3\text{O}$ $[\text{M} + \text{H}]^+$).

4-Isopropyl-2-phenyl-6-(3-(pyrrolidin-1-yl)propoxy)pyrimidine (81). A pale-red oil (1.38 g, 84.5%). ^1H NMR (600 MHz, CDCl_3) δ 8.50–8.44 (m, 2H), 7.50–7.41 (m, 3H), 6.46 (s, 1H), 4.54 (t, J = 6.5 Hz, 2H), 3.03–2.93 (m, 1H), 2.69–2.61 (m, 2H), 2.60–2.57 (m, 4H), 2.09–2.02 (m, 2H), 1.85–1.76 (m, 4H), 1.32 (d, J = 6.9 Hz, 6H). MS (ESI) m/z 326.3 (calcd 326.4 for $\text{C}_{20}\text{H}_{27}\text{N}_3\text{O}$ $[\text{M} + \text{H}]^+$).

4-Methoxy-2-phenyl-6-(3-(pyrrolidin-1-yl)propoxy)pyrimidine (82). A pale-red oil (1.28 g, 81.7%). ^1H NMR (600 MHz, CDCl_3) δ 8.45–8.38 (m, 2H), 7.48–7.44 (m, 3H), 6.75 (s, 1H), 4.56 (t, J = 6.5 Hz, 2H), 3.51 (s, 3H), 2.70–2.62 (m, 2H), 2.60–2.53 (m, 4H), 2.12–2.02 (m, 2H), 1.84–1.76 (m, 4H). MS (ESI) m/z 314.8 (calcd 314.4 for $\text{C}_{18}\text{H}_{23}\text{N}_3\text{O}_2$ $[\text{M} + \text{H}]^+$).

2-Phenyl-4-(3-(pyrrolidin-1-yl)propoxy)-6-(trifluoromethyl)pyrimidine (83). A pale-red oil (1.57 g, 89.6%). ^1H NMR (600 MHz, CDCl_3) δ 8.50–8.42 (m, 2H), 7.53–7.43 (m, 3H), 6.91 (s, 1H), 4.62 (t, J = 6.5 Hz, 2H), 2.69–2.62 (m, 2H), 2.59–2.52 (m, 4H), 2.12–2.04 (m, 2H), 1.84–1.77 (m, 4H). MS (ESI) m/z 352.5 (calcd 352.4 for $\text{C}_{18}\text{H}_{20}\text{F}_3\text{N}_3\text{O}$ $[\text{M} + \text{H}]^+$).

4-Cyclopropyl-2-phenyl-6-(3-(pyrrolidin-1-yl)propoxy)pyrimidine (84). A pale-red oil (1.42 g, 88.1%). ^1H NMR (600 MHz, CDCl_3) δ 8.44–8.37 (m, 2H), 7.59–7.47 (m, 3H), 6.41 (s, 1H), 4.52 (t, J = 6.5 Hz, 2H), 2.54–2.34 (m, 6H), 2.03–1.82 (m, 3H), 1.86–1.73 (m, 4H), 1.30–1.14 (m, 2H), 1.12–1.02 (m, 2H). MS (ESI) m/z 324.6 (calcd 324.4 for $\text{C}_{20}\text{H}_{25}\text{N}_3\text{O}$ $[\text{M} + \text{H}]^+$).

2,4-Diphenyl-6-(3-(pyrrolidin-1-yl)propoxy)pyrimidine (85). A pale-red oil (1.66 g, 92.2%). ^1H NMR (600 MHz, CDCl_3) δ 8.64–8.55 (m, 2H), 8.23–8.18 (m, 2H), 7.58–7.47 (m, 6H), 7.03 (s, 1H), 4.56 (t, J = 6.5 Hz, 2H), 2.56–2.37 (m, 6H), 2.08–1.99 (m, 2H), 1.82–1.70 (m, 4H). MS (ESI) m/z 360.3 (calcd 360.5 for $\text{C}_{23}\text{H}_{25}\text{N}_3\text{O}$ $[\text{M} + \text{H}]^+$).

4,5-Dimethyl-2-phenyl-6-(3-(pyrrolidin-1-yl)propoxy)pyrimidine (86). A pale-red oil (1.33 g, 85.3%). ^1H NMR (600 MHz, CDCl_3) δ 8.43–8.37 (m, 2H), 7.48–7.39 (m, 3H), 4.53 (t, J = 6.4 Hz, 2H), 2.66–2.60 (m, 2H), 2.57–2.50 (m, 4H), 2.47 (s, 3H), 2.13 (s, 3H), 2.08–2.01 (m, 2H), 1.85–1.73 (m, 4H). MS (ESI) m/z 312.8 (calcd 312.4 for $\text{C}_{20}\text{H}_{25}\text{N}_3\text{O}$ $[\text{M} + \text{H}]^+$).

5-Fluoro-4-methyl-2-phenyl-6-(3-(pyrrolidin-1-yl)propoxy)pyrimidine (87). A pale-red oil (1.31 g, 83.1%). ^1H NMR (600 MHz, CDCl_3) δ 8.39–8.29 (m, 2H), 7.49–7.40 (m, 3H), 4.61 (t, J = 6.5 Hz, 2H), 2.69–2.63 (m, 2H), 2.59–2.47 (m, 7H), 2.13–2.03 (m, 2H), 1.85–1.75 (m, 4H). MS (ESI) m/z 316.7 (calcd 316.4 for $\text{C}_{18}\text{H}_{22}\text{FN}_3\text{O}$ $[\text{M} + \text{H}]^+$).

5-Chloro-4-methyl-2-phenyl-6-(3-(pyrrolidin-1-yl)propoxy)pyrimidine (88). A pale-red oil (1.37 g, 82.5%). ^1H NMR (600 MHz, CDCl_3) δ 8.42–8.33 (m, 2H), 7.49–7.42 (m, 3H), 4.61 (t, J = 6.5 Hz, 2H), 2.71–2.65 (m, 2H), 2.63–2.52 (m, 7H), 2.14–2.06 (m, 2H), 1.86–1.75 (m, 4H). MS (ESI) m/z 332.9 (calcd 332.8 for $\text{C}_{18}\text{H}_{22}\text{ClN}_3\text{O}$ $[\text{M} + \text{H}]^+$).

2-Phenyl-6,7-dihydro-5H-cyclopenta[d]pyrimidin-4-ol (91).⁶⁰ To a suspension of benzimidamide hydrochloride (**5**, 50 mmol) and ethyl 2-oxocyclopentanecarboxylate (**89**, 55 mmol) in MeOH (200 mL) was added *t*-BuOK (10 mmol) portionwise, with stirring, at 0 °C for 30 min. The resulting mixture was heated to reflux for 4 h and then cooled down to room temperature. After that, ice–water (200 mL) was added and neutralized with citric acid. The precipitate thus formed was filtered and washed with water. The crude residue obtained was recrystallized from *i*-PrOH to give 2-phenyl-6,7-dihydro-5H-cyclopenta[d]pyrimidin-4-ol, **91**, as a white solid (8.6 g, 81.0%), mp 232–235 °C. ^1H NMR (600 MHz, CDCl_3) δ 12.61 (s, 1H), 8.26–8.07 (m, 2H), 7.60–7.44 (m, 3H), 2.97 (t, J = 7.8 Hz, 2H), 2.88 (t, J = 7.5 Hz, 2H), 2.24–2.05 (m, 2H).

2-Phenyl-5,6,7,8-tetrahydroquinazolin-4-ol (92).⁶⁰ To a suspension of benzimidamide hydrochloride (**5**, 50 mmol) and ethyl 2-oxocyclohexanecarboxylate (**90**, 55 mmol) in MeOH (200 mL) was added *t*-BuOK (10 mmol) portionwise, with stirring, at 0 °C for 30 min. The resulting mixture was heated to reflux for 4 h and then cooled down to room temperature. After that, ice–water (200 mL) was added and neutralized with citric acid. The precipitate thus formed was filtered and washed with water. The crude residue obtained was recrystallized from *i*-PrOH to give 2-phenyl-5,6,7,8-tetrahydroquinazolin-4-ol, **92**, as a white solid (8.9 g, 78.7%), mp 246–249 °C. ^1H NMR (600 MHz, CDCl_3) δ 12.90 (s, 1H), 8.32–8.09 (m, 2H), 7.70–7.36 (m, 3H), 2.74 (t, J = 6.1 Hz, 2H), 2.59 (t, J = 6.0 Hz, 2H), 1.93–1.71 (m, 4H).

2-Phenyl-4-(3-(piperidin-1-yl)propoxy)-6,7-dihydro-5H-cyclopenta[d]pyrimidine (94). To a solution of **91** (10 mmol) and 1,3-dibromopropane (20 mmol) in acetone (100 mL), potassium carbonate (20 mmol) was added and the mixture was refluxed for 4–6 h. The progress of the reaction was monitored by TLC. After cooling to room temperature, the mixture was filtered and the solvent was evaporated under reduced pressure. The crude product was purified by means of chromatography (petroleum ether/EtOAc = 100/1 to 50/1) to yield 4-(3-bromopropoxy)-2-phenyl-6,7-dihydro-5H-cyclopenta[d]pyrimidine, **93**, as a pale-yellow oil (2.17 g, 65.3%). ^1H NMR (600 MHz, CDCl_3) δ 8.47–8.36 (m, 2H), 7.52–7.40 (m, 3H), 4.67 (t, J = 6.0 Hz, 2H), 3.59 (t, J = 6.6 Hz, 2H), 3.03 (t, J = 7.8 Hz, 2H), 2.87 (t, J = 7.5 Hz, 2H), 2.45–2.35 (m, 2H), 2.20–2.10 (m, 2H). MS (ESI) m/z 334.3 (calcd 334.2 for $\text{C}_{16}\text{H}_{17}\text{BrN}_2\text{O}$ $[\text{M} + \text{H}]^+$).

A mixture of **93** (5 mmol) and piperidine (5.5 mmol) in acetonitrile (100 mL) and cesium carbonate (10 mmol) was heated and refluxed for 6–8 h. After filtering, the resulting filtrate was evaporated to dryness under reduced pressure. The residue was suspended in water (50 mL) and extracted with dichloromethane (3×25 mL). The combined organic layers were dried with anhydrous magnesium sulfate, the filtrate evaporated under reduced pressure, and the crude product purified by means of chromatography (10% MeOH/ CHCl_3) to yield 2-phenyl-4-(3-(piperidin-1-yl)propoxy)-6,7-dihydro-5H-cyclopenta[d]pyrimidine, **94**, as a yellow oil (1.27 g, 75.6%). ^1H NMR (600 MHz, CDCl_3) δ 8.44–8.31 (m, 2H), 7.53–7.40 (m, 3H), 4.56 (t, J = 6.5 Hz, 2H), 2.87 (t, J = 6.2 Hz, 2H), 2.68–2.63 (m, 2H), 2.61–2.48 (m, 6H), 2.41–2.36 (m, 2H), 2.08–2.00 (m, 2H), 1.67–1.54 (m, 4H), 1.47–1.41 (m, 2H). MS (ESI) m/z 338.6 (calcd 338.5 for $\text{C}_{21}\text{H}_{27}\text{N}_3\text{O}$ $[\text{M} + \text{H}]^+$).

2-Phenyl-4-(3-(pyrrolidin-1-yl)propoxy)-6,7-dihydro-5H-cyclopenta[d]pyrimidine (95). A mixture of **93** (5 mmol) and pyrrolidine (5.5 mmol) in acetonitrile (100 mL) and cesium carbonate

(10 mmol) was heated and refluxed for 6–8 h. After filtering, the resulting filtrate was evaporated to dryness under reduced pressure. The residue was suspended in water (50 mL) and extracted with dichloromethane (3 × 25 mL). The combined organic layers were dried with anhydrous magnesium sulfate, the filtrate evaporated under reduced pressure, and the crude product purified by means of chromatography (10% MeOH/CHCl₃) to yield 2-phenyl-4-(3-(pyrrolidin-1-yl)propoxy)-6,7-dihydro-5H-cyclopenta[d]pyrimidine, **95**, as a pale-red oil (1.13 g, 70.2%). ¹H NMR (600 MHz, CDCl₃) δ 8.45–8.29 (m, 2H), 7.52–7.40 (m, 3H), 4.57 (t, *J* = 6.5 Hz, 2H), 2.88 (t, *J* = 6.2 Hz, 2H), 2.69–2.64 (m, 2H), 2.63–2.51 (m, 6H), 2.42–2.35 (m, 2H), 2.06–2.00 (m, 2H), 1.85–1.73 (m, 4H). MS (ESI) *m/z* 324.5 (calcd 324.4 for C₂₀H₂₅N₃O [M + H]⁺).

2-Phenyl-4-(3-(piperidin-1-yl)propoxy)-5,6,7,8-tetrahydroquinazoline (97). To a solution of **92** (10 mmol) and 1,3-dibromopropane (20 mmol) in acetone (100 mL), potassium carbonate (20 mmol) was added and the mixture was refluxed for 4–6 h. The progress of the reaction was monitored by TLC. After cooling to room temperature, the mixture was filtered and the solvent was evaporated under reduced pressure. The crude product was purified by means of chromatography (petroleum ether/EtOAc = 100/1 to 50/1) to yield 4-(3-bromopropoxy)-2-phenyl-5,6,7,8-tetrahydroquinazoline, **96**, as a pale-yellow oil (1.90 g, 54.9%). ¹H NMR (600 MHz, CDCl₃) δ 8.42–8.34 (m, 2H), 7.47–7.41 (m, 3H), 4.64 (t, *J* = 5.9 Hz, 2H), 3.59 (t, *J* = 6.6 Hz, 2H), 2.86 (t, *J* = 6.2 Hz, 2H), 2.60 (t, *J* = 6.2 Hz, 2H), 2.43–2.34 (m, 2H), 1.94–1.77 (m, 4H). MS (ESI) *m/z* 348.8 (calcd 348.2 for C₁₇H₁₉BrN₂O [M + H]⁺).

A mixture of **96** (5 mmol) and piperidine (5.5 mmol) in acetonitrile (100 mL) and cesium carbonate (10 mmol) was heated and refluxed for 6–8 h. After filtering, the resulting filtrate was evaporated to dryness under reduced pressure. The residue was suspended in water (50 mL) and extracted with dichloromethane (3 × 25 mL). The combined organic layers were dried with anhydrous magnesium sulfate, the filtrate evaporated under reduced pressure, and the crude product purified by means of chromatography (10% MeOH/CHCl₃) to yield 2-phenyl-4-(3-(piperidin-1-yl)propoxy)-5,6,7,8-tetrahydroquinazoline, **97**, as a yellow oil (1.47 g, 84.0%). ¹H NMR (600 MHz, CDCl₃) δ 8.46–8.32 (m, 2H), 7.51–7.38 (m, 3H), 4.57 (t, *J* = 6.5 Hz, 2H), 2.86 (t, *J* = 6.2 Hz, 2H), 2.68–2.64 (m, 2H), 2.63–2.50 (m, 6H), 2.08–2.00 (m, 2H), 1.92–1.84 (m, 4H), 1.65–1.52 (m, 4H), 1.46–1.40 (m, 2H). MS (ESI) *m/z* 352.7 (calcd 352.5 for C₂₂H₂₉N₃O [M + H]⁺).

2-Phenyl-4-(3-(pyrrolidin-1-yl)propoxy)-5,6,7,8-tetrahydroquinazoline (98). A mixture of **96** (5 mmol) and pyrrolidine (5.5 mmol) in acetonitrile (100 mL) and cesium carbonate (10 mmol) was heated and refluxed for 6–8 h. After filtering, the resulting filtrate was evaporated to dryness under reduced pressure. The residue was suspended in water (50 mL) and extracted with dichloromethane (3 × 25 mL). The combined organic layers were dried with anhydrous magnesium sulfate, the filtrate evaporated under reduced pressure, and the crude product purified by means of chromatography (10% MeOH/CHCl₃) to yield 2-phenyl-4-(3-(pyrrolidin-1-yl)propoxy)-5,6,7,8-tetrahydroquinazoline, **98**, as a pale-red oil (1.30 g, 77.4%). ¹H NMR (600 MHz, CDCl₃) δ 8.44–8.32 (m, 2H), 7.49–7.36 (m, 3H), 4.55 (t, *J* = 6.4 Hz, 2H), 2.85 (t, *J* = 6.2 Hz, 2H), 2.68–2.62 (m, 2H), 2.60–2.48 (m, 6H), 2.10–2.01 (m, 2H), 1.92–1.73 (m, 8H). MS (ESI) *m/z* 338.7 (calcd 338.5 for C₂₁H₂₇N₃O [M + H]⁺).

General Procedures for the Synthesis of 5-Chloro-6-methylpyrimidin-4-ol Derivatives (110–120). **5-Chloro-6-methyl-2-(*p*-tolyl)pyrimidin-4-ol (110).** To a suspension of 4-methylbenzimidamide (**99**, 50 mmol) and ethyl 2-chloro-3-oxobutanoate (**48**, 55 mmol) in MeOH (200 mL) was added *t*-BuOK (10 mmol) portionwise, with stirring, at 0 °C for 30 min. The resulting mixture was heated to reflux for 4 h and then cooled down to room temperature. After that, ice-water (200 mL) was added and neutralized with citric acid. The precipitate thus formed was filtered and washed with water. The crude residue obtained was recrystallized from *i*-PrOH to give 5-chloro-6-methyl-2-(*p*-tolyl)pyrimidin-4-ol, **110**, as a white solid (9.60 g, 81.8%), mp 175–178 °C. ¹H NMR (600 MHz, CDCl₃) δ 11.60 (s, 1H), 8.26

(d, *J* = 8.2 Hz, 2H), 7.24 (d, *J* = 8.2 Hz, 2H), 2.58 (s, 3H), 2.40 (s, 3H).

5-Chloro-2-(4-methoxyphenyl)-6-methylpyrimidin-4-ol (111). A white solid (10.12 g, 80.8%), mp 143–146 °C. ¹H NMR (600 MHz, CDCl₃) δ 11.58 (s, 1H), 8.33 (d, *J* = 8.8 Hz, 2H), 6.95 (d, *J* = 8.9 Hz, 2H), 3.87 (s, 3H), 2.58 (s, 3H).

5-Chloro-6-methyl-2-(4-(trifluoromethyl)phenyl)pyrimidin-4-ol (112).⁶¹ A white solid (12.87 g, 89.2%), mp 157–161 °C. ¹H NMR (600 MHz, CDCl₃) δ 11.60 (s, 1H), 8.50 (d, *J* = 8.2 Hz, 2H), 7.69 (d, *J* = 8.3 Hz, 2H), 2.60 (s, 3H).

5-Chloro-2-(4-fluorophenyl)-6-methylpyrimidin-4-ol (113). A white solid (10.07 g, 84.4%), mp 164–167 °C. ¹H NMR (600 MHz, CDCl₃) δ 12.05 (s, 1H), 8.25–7.98 (m, 2H), 7.24–7.12 (m, 2H), 2.51 (s, 3H).

5-Chloro-2-(3,4-difluorophenyl)-6-methylpyrimidin-4-ol (114). A white solid (11.04 g, 86.1%), mp 170–173 °C. ¹H NMR (600 MHz, CDCl₃) δ 12.78 (s, 1H), 8.25–8.20 (m, 1H), 8.19–8.13 (m, 1H), 7.30–7.15 (m, 1H), 2.58 (s, 3H).

5-Chloro-2-(4-chlorophenyl)-6-methylpyrimidin-4-ol (115). A white solid (10.66 g, 83.6%), mp 171–174 °C. ¹H NMR (600 MHz, CDCl₃) δ 11.84 (s, 1H), 8.44–8.30 (m, 2H), 7.48–7.35 (m, 2H), 2.60 (s, 3H).

5-Chloro-2-(3,4-dichlorophenyl)-6-methylpyrimidin-4-ol (116). A white solid (12.87 g, 88.9%), mp 177–180 °C. ¹H NMR (600 MHz, CDCl₃) δ 11.92 (s, 1H), 8.50–8.45 (m, 1H), 8.27–8.20 (m, 1H), 7.56–7.48 (m, 1H), 2.59 (s, 3H).

5-Chloro-6-methyl-2-(naphthalen-2-yl)pyrimidin-4-ol (117). A white solid (12.41 g, 91.7%), mp 204–207 °C. ¹H NMR (600 MHz, CDCl₃) δ 12.08 (s, 1H), 8.92 (s, 1H), 8.52–8.42 (m, 1H), 8.05–7.95 (m, 1H), 7.93–7.88 (m, 1H), 7.86–7.82 (m, 1H), 7.57–7.49 (m, 2H), 2.63 (s, 3H).

5-Chloro-6-methylpyrimidin-4-ol (118).⁶² To a suspension of formimidamide hydrochloride (**107**, 100 mmol) and ethyl 2-chloro-3-oxobutanoate (**48**, 110 mmol) in MeOH (300 mL) was added *t*-BuOK (20 mmol) portionwise, with stirring, at 0 °C for 30 min. The resulting mixture was heated to reflux for and then cooled down to room temperature. After that, ice-water (500 mL) was added and neutralized with citric acid. The mixture was extracted with EtOH (3 × 150 mL), and the combined organic layers were dried with anhydrous magnesium sulfate. The filtrate was evaporated under reduced pressure, and the crude product was purified by means of chromatography (petroleum ether/EtOAc = 20/1 to 2/1) to yield 5-chloro-6-methylpyrimidin-4-ol, **118**, as a pale-yellow solid (7.56 g, 53.2%), mp 211–213 °C. ¹H NMR (600 MHz, CDCl₃) δ 13.34 (s, 1H), 8.11 (s, 1H), 2.52 (s, 3H).

5-Chloro-2,6-dimethylpyrimidin-4-ol (119).⁶³ A white solid (9.32 g, 58.8%), mp 121–124 °C. ¹H NMR (600 MHz, CDCl₃) δ 13.31 (s, 1H), 2.50 (s, 3H), 2.45 (s, 3H).

5-Chloro-2-cyclopropyl-6-methylpyrimidin-4-ol (120). A white solid (11.50 g, 62.3%), mp 133–136 °C. ¹H NMR (600 MHz, CDCl₃) δ 13.45 (s, 1H), 2.39 (s, 3H), 2.00–1.91 (m, 1H), 1.24–1.18 (m, 2H), 1.14–1.09 (m, 2H).

4-(3-Bromopropoxy)-5-chloro-6-methyl-2-(*p*-tolyl)pyrimidine (121). To a solution of **110** (10 mmol) and 1,3-dibromopropane (20 mmol) in acetone (100 mL), potassium carbonate (20 mmol) was added and the mixture was refluxed for 4–6 h. The progress of the reaction was monitored by TLC. After cooling to room temperature, the mixture was filtered and the solvent was evaporated under reduced pressure. The crude product was purified by means of chromatography (petroleum ether/EtOAc = 100/1 to 50/1) to yield 4-(3-bromopropoxy)-5-chloro-6-methyl-2-(*p*-tolyl)pyrimidine, **121**, as a pale-yellow oil (1.66 g, 46.8%). ¹H NMR (600 MHz, CDCl₃) δ 8.26 (d, *J* = 8.2 Hz, 2H), 7.24 (d, *J* = 8.2 Hz, 2H), 4.65 (t, *J* = 6.0 Hz, 2H), 3.60 (t, *J* = 6.5 Hz, 2H), 2.58 (s, 3H), 2.46–2.33 (m, 5H). MS (ESI) *m/z* 356.8 (calcd 356.7 for C₁₅H₁₆BrClN₂O [M + H]⁺).

4-(3-Bromopropoxy)-5-chloro-2-(4-methoxyphenyl)-6-methylpyrimidine (122). A pale-yellow oil (1.64 g, 44.1%). ¹H NMR (600 MHz, CDCl₃) δ 8.33 (d, *J* = 8.8 Hz, 2H), 6.95 (d, *J* = 8.9 Hz, 2H), 4.65 (t, *J* = 6.0 Hz, 2H), 3.86 (s, 3H), 3.61 (t, *J* = 6.5 Hz, 2H), 2.58 (s,

3H), 2.44–2.35 (m, 2H). MS (ESI) m/z 372.4 (calcd 372.7 for $C_{15}H_{16}BrClN_2O_2$ $[M + H]^+$).

4-(3-Bromopropoxy)-5-chloro-6-methyl-2-(4-(trifluoromethyl)phenyl)pyrimidine (123). A pale-yellow oil (2.15 g, 52.6%). 1H NMR (600 MHz, $CDCl_3$) δ 8.50 (d, J = 8.2 Hz, 2H), 7.70 (d, J = 8.3 Hz, 2H), 4.69 (t, J = 6.0 Hz, 2H), 3.63 (t, J = 6.4 Hz, 2H), 2.62 (s, 3H), 2.50–2.35 (m, 2H). MS (ESI) m/z 410.7 (calcd 410.6 for $C_{15}H_{13}BrClF_3N_2O$ $[M + H]^+$).

4-(3-Bromopropoxy)-5-chloro-2-(4-fluorophenyl)-6-methylpyrimidine (124). A pale-yellow oil (1.75 g, 48.7%). 1H NMR (600 MHz, $CDCl_3$) δ 8.44–8.34 (m, 2H), 7.18–7.06 (m, 2H), 4.66 (t, J = 6.0 Hz, 2H), 3.62 (t, J = 6.4 Hz, 2H), 2.59 (s, 3H), 2.44–2.35 (m, 2H). MS (ESI) m/z 360.6 (calcd 360.6 for $C_{14}H_{13}BrClFN_2O$ $[M + H]^+$).

4-(3-Bromopropoxy)-5-chloro-2-(3,4-difluorophenyl)-6-methylpyrimidine (125). A pale-yellow oil (1.95 g, 51.8%). 1H NMR (600 MHz, $CDCl_3$) δ 8.25–8.19 (m, 1H), 8.19–8.14 (m, 1H), 7.30–7.16 (m, 1H), 4.67 (t, J = 6.0 Hz, 2H), 3.62 (t, J = 6.4 Hz, 2H), 2.60 (s, 3H), 2.46–2.36 (m, 2H). MS (ESI) m/z 378.8 (calcd 378.6 for $C_{14}H_{12}BrClF_2N_2O$ $[M + H]^+$).

5-Chloro-2-(4-chlorophenyl)-4-methyl-6-(3-(piperidin-1-yl)propoxy)pyrimidine (126). A pale-yellow oil (1.85 g, 49.2%). 1H NMR (600 MHz, $CDCl_3$) δ 8.42–8.29 (m, 2H), 7.50–7.36 (m, 2H), 4.69 (t, J = 6.0 Hz, 2H), 3.62 (t, J = 6.4 Hz, 2H), 2.61 (s, 3H), 2.47–2.33 (m, 2H). MS (ESI) m/z 377.2 (calcd 377.1 for $C_{14}H_{13}BrCl_2N_2O$ $[M + H]^+$).

4-(3-Bromopropoxy)-5-chloro-2-(3,4-dichlorophenyl)-6-methylpyrimidine (127). A pale-yellow oil (2.19 g, 53.3%). 1H NMR (600 MHz, $CDCl_3$) δ 8.51–8.45 (m, 1H), 8.26–8.19 (m, 1H), 7.55–7.48 (m, 1H), 4.68 (t, J = 6.0 Hz, 2H), 3.63 (t, J = 6.4 Hz, 2H), 2.61 (s, 3H), 2.46–2.39 (m, 2H). MS (ESI) m/z 411.7 (calcd 411.5 for $C_{14}H_{12}BrCl_3N_2O$ $[M + H]^+$).

4-(3-Bromopropoxy)-5-chloro-6-methyl-2-(naphthalen-2-yl)pyrimidine (128). A pale-yellow oil (2.20 g, 56.2%). 1H NMR (600 MHz, $CDCl_3$) δ 8.92 (s, 1H), 8.53–8.42 (m, 1H), 8.03–7.95 (m, 1H), 7.93–7.89 (m, 1H), 7.88–7.84 (m, 1H), 7.57–7.47 (m, 2H), 4.75 (t, J = 6.0 Hz, 2H), 3.65 (t, J = 6.4 Hz, 2H), 2.65 (s, 3H), 2.51–2.39 (m, 2H). MS (ESI) m/z 392.9 (calcd 392.7 for $C_{18}H_{16}BrClN_2O$ $[M + H]^+$).

4-(3-Bromopropoxy)-5-chloro-6-methylpyrimidine (129). A pale-yellow oil (1.07 g, 40.2%). 1H NMR (600 MHz, $CDCl_3$) δ 8.33 (s, 1H), 4.24 (t, J = 6.0 Hz, 2H), 3.62 (t, J = 6.4 Hz, 2H), 2.48 (s, 3H), 2.34–2.25 (m, 2H). MS (ESI) m/z 267.1 (calcd 266.5 for $C_8H_{10}BrClN_2O$ $[M + H]^+$).

4-(3-Bromopropoxy)-5-chloro-2,6-dimethylpyrimidine (130). A pale-yellow oil (1.20 g, 42.9%). 1H NMR (600 MHz, $CDCl_3$) δ 4.18 (t, J = 6.0 Hz, 2H), 3.51 (t, J = 6.1 Hz, 2H), 2.60 (s, 3H), 2.39 (s, 3H), 2.34–2.25 (m, 2H). MS (ESI) m/z 280.8 (calcd 280.6 for $C_9H_{12}BrClN_2O$ $[M + H]^+$).

4-(3-Bromopropoxy)-5-chloro-2-cyclopropyl-6-methylpyrimidine (131). A pale-yellow oil (1.35 g, 44.5%). 1H NMR (600 MHz, $CDCl_3$) δ 4.20 (t, J = 6.0 Hz, 2H), 3.55 (t, J = 6.2 Hz, 2H), 2.46 (s, 3H), 2.43–2.32 (m, 2H), 1.76–1.70 (m, 1H), 1.26–1.20 (m, 2H), 1.15–1.10 (m, 2H). MS (ESI) m/z 306.9 (calcd 306.6 for $C_{11}H_{14}BrClN_2O$ $[M + H]^+$).

5-Chloro-4-methyl-6-(3-(piperidin-1-yl)propoxy)-2-(p-tolyl)pyrimidine (132). A mixture of **121** (5 mmol) and piperidine (5.5 mmol) in acetonitrile (100 mL) and cesium carbonate (10 mmol) was heated and refluxed for 6–8 h. After filtering, the resulting filtrate was evaporated to dryness under reduced pressure. The residue was suspended in water (50 mL) and extracted with dichloromethane (3 \times 25 mL). The combined organic layers were dried with anhydrous magnesium sulfate, the filtrate evaporated under reduced pressure, and the crude product purified by means of chromatography (10% MeOH/ $CHCl_3$) to yield 5-chloro-4-methyl-6-(3-(piperidin-1-yl)propoxy)-2-(p-tolyl)pyrimidine, **132**, as a yellow oil (1.52 g, 84.8%). 1H NMR (600 MHz, $CDCl_3$) δ 8.26 (d, J = 8.2 Hz, 2H), 7.24 (d, J = 8.0 Hz, 2H), 4.57 (t, J = 6.5 Hz, 2H), 2.58 (s, 3H), 2.54–2.49 (m, 2H), 2.49–2.32 (m, 7H), 2.09–2.01 (m, 2H), 1.63–1.54 (m, 2H), 1.49–1.38 (m, 2H). MS (ESI) m/z 361.2 (calcd 360.9 for $C_{20}H_{26}ClN_3O$ $[M + H]^+$).

5-Chloro-2-(4-methoxyphenyl)-4-methyl-6-(3-(piperidin-1-yl)propoxy)pyrimidine (133). A yellow oil (1.54 g, 82.1%). 1H NMR (600 MHz, $CDCl_3$) δ 8.33 (d, J = 8.9 Hz, 2H), 6.95 (d, J = 8.9 Hz, 2H), 4.57 (t, J = 6.5 Hz, 2H), 3.86 (s, 3H), 2.57 (s, 3H), 2.54–2.49 (m, 2H), 2.48–2.32 (m, 4H), 2.10–2.00 (m, 2H), 1.66–1.52 (m, 4H), 1.50–1.39 (m, 2H). MS (ESI) m/z 377.1 (calcd 375.9 for $C_{20}H_{26}ClN_3O_2$ $[M + H]^+$).

5-Chloro-4-methyl-6-(3-(piperidin-1-yl)propoxy)-2-(4-(trifluoromethyl)phenyl)pyrimidine (134). A yellow oil (1.83 g, 88.7%). 1H NMR (600 MHz, $CDCl_3$) δ 8.48 (d, J = 8.2 Hz, 2H), 7.68 (d, J = 8.3 Hz, 2H), 4.59 (t, J = 6.5 Hz, 2H), 2.60 (s, 3H), 2.55–2.50 (m, 2H), 2.50–2.32 (m, 4H), 2.11–2.04 (m, 2H), 1.65–1.55 (m, 4H), 1.50–1.40 (m, 2H). MS (ESI) m/z 414.9 (calcd 414.9 for $C_{20}H_{23}ClF_3N_3O$ $[M + H]^+$).

5-Chloro-2-(4-fluorophenyl)-4-methyl-6-(3-(piperidin-1-yl)propoxy)pyrimidine (135). A yellow oil (1.46 g, 80.5%). 1H NMR (600 MHz, $CDCl_3$) δ 8.44–8.31 (m, 2H), 7.19–7.01 (m, 2H), 4.57 (t, J = 6.5 Hz, 2H), 2.58 (s, 3H), 2.55–2.48 (m, 2H), 2.47–2.28 (m, 4H), 2.09–2.02 (m, 2H), 1.65–1.54 (m, 4H), 1.51–1.38 (m, 2H). MS (ESI) m/z 365.1 (calcd 364.9 for $C_{19}H_{23}ClFN_3O$ $[M + H]^+$).

5-Chloro-2-(3,4-difluorophenyl)-4-methyl-6-(3-(piperidin-1-yl)propoxy)pyrimidine (136). A yellow oil (1.65 g, 86.6%). 1H NMR (600 MHz, $CDCl_3$) δ 8.21–8.16 (m, 1H), 8.15–8.10 (m, 1H), 7.23–7.16 (m, 1H), 4.55 (t, J = 6.5 Hz, 2H), 2.57 (s, 3H), 2.53–2.48 (m, 2H), 2.47–2.36 (m, 4H), 2.11–1.99 (m, 2H), 1.64–1.55 (m, 4H), 1.49–1.38 (m, 2H). MS (ESI) m/z 383.3 (calcd 382.8 for $C_{19}H_{22}ClF_2N_3O$ $[M + H]^+$).

5-Chloro-2-(4-chlorophenyl)-4-methyl-6-(3-(piperidin-1-yl)propoxy)pyrimidine (137). A yellow oil (1.55 g, 81.6%). 1H NMR (600 MHz, $CDCl_3$) δ 8.38–8.26 (m, 2H), 7.45–7.36 (m, 2H), 4.56 (t, J = 6.5 Hz, 2H), 2.57 (s, 3H), 2.52–2.47 (m, 2H), 2.46–2.34 (m, 4H), 2.09–1.99 (m, 2H), 1.64–1.53 (m, 4H), 1.48–1.40 (m, 2H). MS (ESI) m/z 381.4 (calcd 381.3 for $C_{19}H_{23}Cl_2N_3O$ $[M + H]^+$).

5-Chloro-2-(3,4-dichlorophenyl)-4-methyl-6-(3-(piperidin-1-yl)propoxy)pyrimidine (138). A yellow oil (1.81 g, 87.5%). 1H NMR (600 MHz, $CDCl_3$) δ 8.45–8.43 (m, 1H), 8.21–8.17 (m, 1H), 7.51–7.46 (m, 1H), 4.56 (t, J = 6.5 Hz, 2H), 2.58 (s, 3H), 2.55–2.49 (m, 2H), 2.48–2.36 (m, 4H), 2.10–2.02 (m, 2H), 1.65–1.54 (m, 4H), 1.51–1.40 (m, 2H). MS (ESI) m/z 416.3 (calcd 414.8 for $C_{19}H_{22}Cl_3N_3O$ $[M + H]^+$).

5-Chloro-4-methyl-2-(naphthalen-2-yl)-6-(3-(piperidin-1-yl)propoxy)pyrimidine (139). A yellow oil (1.71 g, 86.4%). 1H NMR (600 MHz, $CDCl_3$) δ 8.89 (s, 1H), 8.54–8.41 (m, 1H), 8.02–7.93 (m, 1H), 7.95–7.90 (m, 1H), 7.86–7.82 (m, 1H), 7.56–7.45 (m, 2H), 4.62 (t, J = 6.5 Hz, 2H), 2.62 (s, 3H), 2.58–2.51 (m, 2H), 2.50–2.28 (m, 4H), 2.13–2.04 (m, 2H), 1.64–1.56 (m, 4H), 1.50–1.41 (m, 2H). MS (ESI) m/z 397.2 (calcd 396.9 for $C_{23}H_{26}ClN_3O$ $[M + H]^+$).

5-Chloro-4-methyl-6-(3-(piperidin-1-yl)propoxy)pyrimidine (140). A yellow oil (1.04 g, 77.3%). 1H NMR (600 MHz, $CDCl_3$) δ 8.53 (s, 1H), 4.28 (t, J = 6.5 Hz, 2H), 2.58 (s, 3H), 2.51–2.45 (m, 2H), 2.47–2.34 (m, 4H), 2.08–1.99 (m, 2H), 1.62–1.55 (m, 4H), 1.47–1.40 (m, 2H). MS (ESI) m/z 271.1 (calcd 270.8 for $C_{13}H_{20}ClN_3O$ $[M + H]^+$).

5-Chloro-2,4-dimethyl-6-(3-(piperidin-1-yl)propoxy)pyrimidine (141). A yellow oil (1.12 g, 79.6%). 1H NMR (600 MHz, $CDCl_3$) δ 4.22 (t, J = 6.5 Hz, 2H), 2.54 (s, 3H), 2.47–2.39 (m, 2H), 2.36–2.28 (m, 7H), 2.03–1.95 (m, 2H), 1.61–1.53 (m, 4H), 1.45–1.38 (m, 2H). MS (ESI) m/z 284.8 (calcd 284.8 for $C_{14}H_{22}ClN_3O$ $[M + H]^+$).

5-Chloro-2-cyclopropyl-4-methyl-6-(3-(piperidin-1-yl)propoxy)pyrimidine (142). A yellow oil (1.24 g, 80.1%). 1H NMR (600 MHz, $CDCl_3$) δ 4.31 (t, J = 6.5 Hz, 2H), 2.56 (s, 3H), 2.48–2.38 (m, 2H), 2.38–2.27 (m, 7H), 2.02–1.94 (m, 2H), 1.75–1.69 (m, 1H), 1.60–1.53 (m, 4H), 1.44–1.36 (m, 2H), 1.25–1.19 (m, 2H), 1.16–1.10 (m, 2H). MS (ESI) m/z 310.5 (calcd 310.8 for $C_{16}H_{24}ClN_3O$ $[M + H]^+$).

In Vitro Binding Assays. Materials. The following specific radioligands and tissue sources were used: (a) σ_1 receptor, [3H]-(+)-pentazocine (250 μ Ci, PerkinElmer, NET-1056250UC), and male Dunkin Hartley guinea pig brain membrane; (b) σ_2 receptor, [3H]-di-*o*-tolylguanidine ([3H]-DTG, 250 μ Ci, PerkinElmer, NET-986250UC), and male Dunkin Hartley guinea pig brain membrane. Chemicals and reagents were purchased from different commercial sources and of analytical grade.

Membrane Preparation. Membrane preparation was performed by previously reported method.⁶⁵ Crude P2 membranes were prepared from frozen guinea pig brains minus cerebellum. Tissues were homogenized in ice-cold 10 mM Tris-sucrose buffer (0.32 mol sucrose in 10 mM Tris-HCl, pH 7.4) using an ULTRA TURAX homogenizer. The homogenates were centrifuged at 4 °C at 1000g for 10 min, and the supernatant was saved. The resulting pellet was then resuspended in the same buffer, incubated for 10 min at 4 °C, and centrifuged at 1000g for 10 min. After that, the pellet was discarded and the supernatants were combined and centrifuged at 31000g for 15 min. The pellets were resuspended in 10 mL of Tris-HCl, pH 7.4, in a volume of 3 mL/g, and the suspension was allowed to incubate at 25 °C for 30 min. Following centrifuging at 31000g for 15 min, the pellet was resuspended by gentle homogenization in 10 mM Tris-HCl, pH 7.4, in a final volume of 1.53 mL/g tissue, and aliquots were stored at -80 °C until used. The protein concentration of the suspension was determined by the method of Bradford.⁶⁶ Subsequently, the preparation contained 4 mg protein/mL.

General Procedures for the Binding Assays. All the test compounds were prepared by dissolving in 5% DMSO. The filter mats were presoaked in 0.5% polyethylenimine solution for 2 h at room temperature before use. The following specific radioligands and tissue sources were used: (a) σ_1 receptor, [³H]-(+)-pentazocine, guinea pig brain membranes; (b) σ_2 receptor, [³H]-DTG, guinea pig brain membranes.

The total binding (TB) was determined in the absence of nonspecific binding and compounds while specific binding (SB) was determined in the presence of compounds. Nonspecific binding (NB) was determined as the difference between total and specific binding. Nonspecific binding was determined in the presence of 10 μ M of haloperidol. Percentage of inhibition (%) was calculated as the following equation:

$$\text{percentage of inhibition(\%)} = (\text{TB} - \text{SB}) / (\text{TB} - \text{NB}) \times 100\%$$

Blank experiments were carried out to determine the effect of 5% DMSO on the binding, and no effects were observed. Compounds were tested at least three times over a six concentration range (10^{-5} M to 10^{-10} M), and IC_{50} values were determined by nonlinear regression analysis using Hill equation curve fitting. K_i values were calculated based on the Cheng and Prusoff equation: $K_i = \text{IC}_{50} / (1 + C/K_d)$. In the equation, C represents the concentration of the hot ligand used and K_d its receptor dissociation constant calculated for each labeled ligand. Mean K_i values and SEM are reported for at least three independent experiments.

σ_1 Receptor Binding Assays. Binding of [³H]-(+)-pentazocine at σ_1 receptor was performed according to D. L. Dehaven-Hudkins et al.,⁵² with minor modifications. The binding properties of the test compounds to guinea pig σ_1 receptor were studied in guinea pig brain membranes using [³H]-(+)-pentazocine as the radioligand.

To each total binding assay tube was added 900 μ L of the tissue suspension, 50 μ L of 4.0 nM [³H]-(+)-pentazocine, 50 μ L of Tris-HCl buffer, pH 8.0. Nonspecific binding each assay tube was added 900 μ L of the tissue suspension, 50 μ L of [³H]-(+)-pentazocine, and 50 μ L of 10 μ M haloperidol. To each specific binding assay tube was added 900 μ L of the tissue suspension, 50 μ L of [³H]-(+)-pentazocine, and 50 μ L of reference drug or test compounds solution in various concentrations (10^{-5} M to 10^{-10} M). The tubes were incubated at 25 °C for 180 min. The incubation was followed by a rapid vacuum filtration through Whatman GF/B glass filters, and the filtrates were washed twice with 5 mL of cold buffer and transferred to scintillation vials. Scintillation fluid (2.0 mL) was added, and the radioactivity bound was measured using a Beckman LS 6500 liquid scintillation counter.

σ_2 Receptor Binding Assays. Binding assays were performed as described by Ronsisvalle et al.⁶⁷ with minor modifications.⁴² The binding properties of the test compounds to guinea pig σ_2 receptor were studied in guinea pig brain membranes using [³H]-DTG.

The membranes were incubated with 3 nM [³H]-DTG in the presence of 400 nM (+)-SKF10047 to block σ_1 sites. To each total binding assay tube was added 850 μ L of the tissue suspension, 50 μ L of 3.0 nM [³H]-DTG, 50 μ L of 400 nM (+)-SKF10047, and 50 μ L of

Tris-HCl buffer, pH 8.0. For nonspecific binding, to each assay tube was added 850 μ L of the tissue suspension, 50 μ L of [³H]-DTG, 50 μ L of 400 nM (+)-SKF10047, and 50 μ L of 10 μ M DTG. Each specific binding assay tube was added 850 μ L of the tissue suspension, 50 μ L of [³H]-DTG, 50 μ L of 400 nM (+)-SKF10047, and 50 μ L of reference drug or test compounds solution in various concentrations (10^{-5} M to 10^{-10} M). The tubes were incubated at 25 °C for 120 min. The incubation was followed by a rapid vacuum filtration through Whatman GF/B glass filters, and the filtrates were washed twice with 5 mL of cold buffer and transferred to scintillation vials. Scintillation fluid (2.0 mL) was added, and the radioactivity bound was measured using a Beckman LS 6500 liquid scintillation counter.

Functional Profile on σ_1 Receptor. The functional activity of compound 137 was evaluated by using guinea pig brain membranes binding assays for σ_1 receptor. The binding affinities either in the absence or presence of 1 mM phenytoin were measured to identify the functional (agonistic or antagonistic) nature.⁴⁸

hERG Affinity. Ability to block hERG potassium channels was determined using the whole-cell patch clamp method and cloned hERG potassium channels (expressed in HEK 293 cells) as biological material.⁴⁷ For this purpose, the patch clamp amplifier (Axopatch 200B, Molecular Devices) and digital converter (Digidata 1440A, Molecular Devices) were used. Recording electrodes were made from borosilicate glass with filament (BF120-94-15, Sutter Instrument Company). Creation of voltage-clamp command pulse protocols and data acquisition were controlled by pCLAMP software (version 10.1, Molecular Devices).

The bath solution consisted of 137 mM NaCl, 5.4 mM KCl, 10 mM glucose, 10 mM HEPES, and 2 mM CaCl₂. The pH was adjusted to 7.5 by addition of NaOH. The pipet filling solution consisted of 140 mM KCl, 1 mM MgCl₂, 5 mM EGTA, 10 mM HEPES, and 5 mM Na₂ATP. The pH was adjusted to 7.2 by addition of KOH.

To study voltage dependence of steady-state block of hERG channels on different drug concentrations (0.3, 1, 3, and 10 μ M) in HEK cells, the holding membrane potential was switched from -80 to +50 mV for 2 s following return to -50 mV for 3 s (sampling rate of 4 kHz, low-pass filtered at 1 kHz) in intervals of 30 s. Tail currents were measured at -50 mV in control and in the presence of the drug at concentrations determined empirically.

All raw measurements were performed using Clampfit (version 10.2), a part of pCLAMP software (version 10.1). Results were transferred to the program Statistical Package for the Social Sciences (SPSS) spreadsheets for further analysis.

In Vivo Test. Animals. Chinese Kun Ming (KM) mice (20 ± 2.0 g) and Sprague-Dawley (SD) rats (250 ± 5.0 g) were used as experimental animals in this study. All the animals were housed under standardized conditions for light, temperature, and humidity and received standard rat chow and tap water and libitum. Animals were assigned to different experimental groups randomly, each kept in a separate cage. All research involving animals in this study follow the guidelines of the Bylaws of Experiments on Animals and have been approved by the Ethics and Experimental Animal Committee of Jiangsu Nhwa Pharmaceutical Co., Ltd.

Acute Toxicity. Mice (10 mice for each group) were orally dosed with po administration of a 10 mL/kg volume of vehicle 0.5% methylcellulose (Sigma-Aldrich) or increasing dose of test compounds (200, 500, 1000, 1500, and 2000 mg/kg). The number of surviving animals was recorded after 24 h of drug administration. The percent mortality in each group was calculated. The LD₅₀ values were calculated by using Statistical Package for Social Sciences (SPSS) program.

Formalin Test.⁴⁴ Mice were randomly separated into different groups: vehicle, vehicle + formalin, and drug-treated group, and each group contained 10 mice. A diluted formalin solution (20 μ L of a 2.5% formalin solution, 0.92% formaldehyde) was injected into the dorsal surface of the right hind paw of the mouse. Immediately thereafter, the mouse was put into a glass cylinder and the observation period started. A mirror was placed behind the glass cylinder to allow clear observation of the paws. Nociceptive behavior induced by formalin was quantified as the time spent licking or biting the injected paw

during two different periods individually recorded: the first period was recorded 0–5 min after the injection of formalin and was considered indicative of formalin-evoked nociception phase I; the second period was recorded 15–45 min after formalin injection and was considered indicative of formalin-evoked nociception phase II.⁴⁴ The mice ($n = 10$ –12 per group) received ip administration of a 10 mL/kg volume of vehicle 30% PEG 400 (Sigma-Aldrich) or test compound 15 min before intraplantar (ipl) formalin injection. The antinociceptive effect induced by the different treatments in the formalin test was calculated by the following formula: antinociceptive effect (%) = $(LT_V - LT_D)/LT_V \times 100\%$, where LT_V represents the licking time in vehicle injected animals and LT_D means licking time in drug-injected animals.

CCI Model.^{50,51} The CCI of the sciatic nerve as an animal model was used to study the efficacy of treatments in neuropathic pain.

Rats were randomly separated into several groups: sham control and vehicle- and drug-treated groups, and each group contained 10 rats. Pain threshold base values of each group were measured 1–2 days before surgery and those with the value of 2 days were picked. The pain thresholds were measured again 14 days after surgery to check whether the model was successful. Drugs were dose orally with po administration of a 10 mL/kg volume of vehicle 0.5% methylcellulose (Sigma-Aldrich) or increasing dose of test compounds twice a day for 4 days (15th, 16th, 17th, and 18th day). Each group was measured after first administration on the 15th day and the last administration on the 18th day, which result in the single administration and repeated administration, respectively.

The CCI of the sciatic nerve surgery was performed as described by Bennett and Xie⁵⁰ with minor modification. Briefly, the SD rats were anesthetized with chloral hydrate (5%) and the right common sciatic nerve was exposed at the level of the mid thigh of the right hind paw. At about 1 cm proximal to the nerve trifurcation, about 7 mm of the nerve was freed and four ligatures (4–0 silk thread) were tight loosely with a distance of ca. 1.0 mm. The nerve was only barely constricted. The muscle was then stitched and the skin incision closed with wound clips. The rats with sciatic nerve exposure without ligation served as the sham control group.

Two tests were performed: the von Frey test and the plantar test. Allodynia to mechanical stimuli and hyperalgesia to noxious thermal stimulus were used as outcome measures of neuropathic pain by using the von Frey and plantar tests, respectively.

In the von Frey test, briefly, animals were placed in a transparent test chamber with a wire-mesh grid floor through which von Frey monofilaments were applied. The monofilaments were applied in increasing force until the rats withdrew the ipsilateral, nerve injury paw using an up–down paradigm. Clear paw withdrawal, sharking, or licking was considered as nociceptive-lick response to determine the mechanical withdrawal threshold (MWT). Animals were adapted to the testing situation for at least 30 min before the sessions started. For each measurement, the paw was sampled four times and a mean calculated. At least 3 min elapsed between.

Thermal hyperalgesia was assessed through the plantar test by measuring hind paw latency in response to radiant heat. Briefly, rats were placed in a clear plastic chamber with a glass floor and allowed to acclimate to the environment for 30 min. A radiant heat source (BMC-410A) was then positioned under the plantar surface of the hind paw. The latency for the withdrawal reflex was recorded as thermal withdraw latency (TWL). A cutoff time of 30 s was imposed to prevent tissue damage in the absence of response. For each measurement, the paw was sampled four times and a mean calculated. At least 3 min elapsed between.

Motor Coordination (Rotarod Test).⁴² The motor performance of mice was assessed by means of an automated rotarod (YLS-4C, China). Mice were trained, and those which could not stay moving on the rod for 300 s in 10 rpm were discarded from the study before drug treatment. In the test, mice were required to walk against the motion of an elevated rotating drum at 10 rpm and the latencies to fall-down were recorded. With the selected animals, rotarod latencies were measured 30, 60, 90, and 120 min after ip administration of drugs.

Pharmacokinetics Study in Rats. The HPLC conditions were as follows: column, ZORBAX BP-C18 5.0 $\mu\text{m} \times 150 \text{ mm} \times 4.6 \text{ mm}$ I.D.

(Agilent, USA); mobile phase, 30 mmol of NH_4COOH (Roe Scientific Inc., USA) aq/acetonitrile (Merck Company, Germany) 30/70; flow rate, 1.0 mL/min; column temperature, 40 °C.

For routine compound 137 screening, rats ($n = 8/\text{group}$) were dosed via the lateral tail vein at the indicated dose for iv administration (16 mg/kg, 100% saline) or via oral gavage (320 mg/kg, suspension in 0.5% methylcellulose). At 30 min, 1, 2, 3, 4, 5, 6, 7, and 24 h after administration, serial blood samples were collected from the lateral tail vein into heparinized collection tubes (approximately 0.25 mL). The plasma was separated by centrifugation, and the sample was prepared for HPLC/MS analysis by protein precipitation with acetonitrile. The plasma samples were analyzed for drug and internal standard via the HPLC-MS/MS protocol.

■ ASSOCIATED CONTENT

● Supporting Information

Details of computational procedures, selectivity of compound 137 for additional receptors and ion channels, inhibition curves figure of functional profile of σ_1 receptor, ^{13}C NMR and HR-MS of partially new compounds, and ^1H NMR, ^{13}C NMR, HR-MS, LC-MS, and elemental analyses of compound 137. This material is available free of charge via the Internet at <http://pubs.acs.org>.

■ AUTHOR INFORMATION

Corresponding Author

*Phone: +86-27-87792235. Fax: +86-27-87792170. E-mail: gszhang@mail.hust.edu.cn.

Author Contributions

[§]Y.L. and Y.C. contributed equally to this work;

Notes

The authors declare no competing financial interest.

■ ACKNOWLEDGMENTS

We thank Prof. Liangren Zhang, Zhenming Liu, and Hongwei Jin of the State Key Laboratory of Natural and Biomimetic Drugs, School of Pharmaceutical Sciences, Peking University, for guiding computational works of 3D Pharmacophore Model Generation, molecular design, and performing HR-MS and elemental analyses for partially new compounds.

■ ABBREVIATIONS USED

$\sigma_1\text{R}$, sigma-1 receptor; $\sigma_2\text{R}$, sigma-2 receptor; CNS, central nervous system; NMDA, N-methyl-D-aspartate; 3D, three-dimensional; hERG, ether-a-go-go-related gene; CCI, chronic constriction injury; ED_{50} , 50% effective dose; LD_{50} , median lethal dose

■ REFERENCES

- (1) Hecke, O. V.; Austin, S. K.; Khan, R. A.; Smith, B. H.; Torrance, N. Neuropathic Pain in the General Population: A Systematic Review of Epidemiological Studies. *Pain* **2014**, *155*, 654–662.
- (2) Gilron, I.; Dickenson, A. H. Emerging Drugs for Neuropathic Pain. *Expert Opin. Emerging Drugs* **2014**, *19*, 1–13.
- (3) Jongen Joost, L. M.; Hans, G.; Benzon, H. T.; Huygen, F.; Hartrick, C. T. Neuropathic Pain and Pharmacological Treatment. *Pain Pract.* **2014**, *14*, 283–295.
- (4) Dworkin, R. H.; O'Connor, A. B.; Backonja, M.; Farrar, J. T.; Finnerup, N. B.; Jensen, T. S.; Kalso, E. A.; Loeser, J. D.; Miaskowski, C.; Nurmikko, T. J.; Portenoy, R. K.; Rice, A. S.; Stacey, B. R.; Treede, R. D.; Turk, D. C.; Wallace, M. S. Pharmacologic Management of Neuropathic Pain: Evidence-Based Recommendations. *Pain* **2007**, *132*, 237–251.
- (5) Attal, N.; Cruccu, G.; Baron, R.; Haanpää, M.; Hansson, P.; Jensen, T. S.; Nurmikko, T. EFNS Guidelines on Pharmacological

Treatment of Neuropathic Pain: 2010 Revision. *Eur. J. Neurol.* **2006**, *13*, 1153–1169.

(6) Moulin, D. E.; Clark, A. J.; Gilron, I.; Ware, M. A.; Watson, C. P.; Sessle, B. J.; Coderre, T.; Morley-Forster, P. K.; Stinson, J.; Boulanger, A.; Peng, P.; Finley, G. A.; Taenzer, P.; Squire, P.; Dion, D.; Cholkkan, A.; Gilani, A.; Gordon, A.; Henry, J.; Jovey, R.; Lynch, M.; Mailis-Gagnon, A.; Panju, A.; Rollman, G. B.; Velly, A. Pharmacological Management of Chronic Neuropathic Pain—Consensus Statement and Guidelines from the Canadian Pain Society. *Pain Res. Manage.* **2007**, *12*, 13–21.

(7) O'Connor, A. B.; Dworkin, R. H. Treatment of Neuropathic Pain: An Overview of Recent Guidelines. *Am. J. Med.* **2009**, *122*, s22–s32.

(8) Cohen, S. P.; Mao, J. R. Neuropathic Pain: Mechanisms and Their Clinical Implications. *Br. Med. J.* **2014**, *348*, f7656.

(9) Vranken, J. H. Elucidation of Pathophysiology and Treatment of Neuropathic Pain. *Cent. Nerv. Syst. Agents Med. Chem.* **2012**, *12*, 304–314.

(10) Dworkin, R. H.; O'Connor, A. B.; Audette, J.; Baron, R.; Gourlay, G. K.; Haanpää, M. L.; Kent, J. L.; Krane, E. J.; Lebel, A. A.; Levy, R. M.; Mackey, S. C.; Mayer, J.; Miaskowski, C.; Raja, S. N.; Rice, A. S.; Schmader, K. E.; Stacey, B.; Stanos, S.; Treede, R. D.; Turk, D. C.; Walco, G. A.; Wells, C. D. Recommendations for the Pharmacological Management of Neuropathic Pain: An Overview and Literature Update. *Mayo Clin. Proc.* **2010**, *85*, s3–s14.

(11) Martin, W. R.; Eades, C. G.; Thompson, J. A.; Huppler, R. E.; Gilbert, P. E. The Effects of Morphine- and Nalorphine-Like Drugs in the Nondependent and Morphine-Dependent Chronic Spinal Dog. *J. Pharmacol. Exp. Ther.* **1976**, *197*, 517–532.

(12) Zukin, S. R.; Brady, K. T.; Slifer, B. L.; Balster, R. L. Behavioral and Biochemical Stereoselectivity of Sigma Opiate/PCP Receptors. *Brain Res.* **1984**, *294*, 174–177.

(13) Mendelsohn, L. G.; Kalra, V.; Johnson, B. G.; Kerchner, G. A. Sigma Opioid Receptor: Characterization and Co-identity with the Phencyclidine Receptor. *J. Pharmacol. Exp. Ther.* **1985**, *233*, 597–602.

(14) Bowen, W. D. Sigma Receptor: Advances and New Clinical Potentials. *Pharm. Acta Helv.* **2000**, *74*, 211–218.

(15) Hellewell, S. B.; Bowen, W. D. A Sigma-like Binding Site in Rat Pheochromocytoma (PC12) Cells: Decreased Affinity for (+)-Benzomorphans and Lower Molecular Weight Suggest a Different Sigma Receptor Form from that in Guinea Pig Brain. *Brain Res.* **1990**, *527*, 244–253.

(16) Quirion, R.; Bowen, W. D.; Itzhak, Y.; Junien, J. L.; Musacchio, J. M.; Rothman, R. B.; Su, T. P.; Tarm, S. W.; Taylor, D. P. A proposal for the classification of sigma binding sites. *Trends Pharmacol. Sci.* **1992**, *13*, 85–86.

(17) Su, T. P.; Hayashi, T. Understanding the Molecular Mechanism of Sigma-1 Receptor: Towards a Hypothesis that Sigma-1 Receptor Are Intracellular Amplifiers for Signal Transduction. *Curr. Med. Chem.* **2003**, *10*, 2073–2080.

(18) Cobos, E. J.; Entrena, J. M.; Cendán, C. M.; Del Pozo, E. Pharmacology and Therapeutic Potential of Sigma-1 Receptor Ligands. *Curr. Neuropharmacol.* **2008**, *6*, 344–366.

(19) Monnet, F. P.; Debonnel, G.; Junien, J. L.; De Montigny, C. N-Methyl-D-aspartate-induced neuronal activation is selectively modulated by sigma receptors. *Eur. J. Pharmacol.* **1990**, *179*, 441–455.

(20) Cheng, Z. X.; Lan, M. D.; Wu, P. X.; Zhu, Y. H.; Dong, Y.; Ma, L.; Zheng, P. Neurosteroid dehydroepiandrosterone sulphate inhibits persistent sodium currents in rat medial prefrontal cortex via activation of sigma-1 receptors. *Exp. Neurol.* **2010**, *210*, 128–136.

(21) Ayder, E.; Palmer, C. P.; Klyachko, V. A.; Jackson, M. B. The Sigma Receptor as A Ligand-Regulated Auxiliary Potassium Channel Subunit. *Neuron* **2002**, *34*, 399–410.

(22) Hayashi, T.; Maurice, T.; Su, T. P. Ca²⁺ Signaling via σ_1 Receptor: Novel Regulatory Mechanism Affecting Intracellular Ca²⁺ Concentration. *J. Pharmacol. Exp. Ther.* **2000**, *293*, 788–798.

(23) Crawford, K. W.; Bowen, W. D. Sigma-2 Receptor Agonists Activate A Novel Apoptotic Pathway and Potentiate Antineoplastic Drugs in Breast Tumor Cell Lines. *Cancer Res.* **2002**, *1*, 313–322.

(24) Mach, R. H.; Zeng, C. B.; Hawkins, W. G. The Sigma-2 Receptor: A Novel Protein for the Imaging and Treatment of Cancer. *J. Med. Chem.* **2013**, *56*, 7137–7160.

(25) Bermack, J. E.; Debonnel, G. The Role of Sigma Receptors in Depression. *J. Pharmacol. Sci.* **2005**, *97*, 317–336.

(26) Ovalle, S.; Andreu, F.; Pérez, M. P.; Zamanillo, D.; Guitart, X. Effect of the Novel Sigma 1 Receptor Ligand and Putative Atypical Antipsychotic E-5842 on BDNF mRNA Expression in the Rat Brain. *NeuroReport* **2002**, *13*, 2345–2348.

(27) Hayashi, T.; Su, T. P. The Potential Role of Sigma-1 Receptor in Lipid Transport and Lipid Raft Reconstitution in the Brain: Implication for Drug Abuse. *Life Sci.* **2005**, *77*, 1612–1624.

(28) Meunier, J.; Gue, M.; Recasens, M.; Maurice, T. Attenuation by A Sigma₁ (σ_1) Receptor Agonist of the Learning and Memory Deficits Induced by a Prenatal Restraint Stress in Juvenile Rats. *Br. J. Pharmacol.* **2004**, *142*, 689–700.

(29) Zamanillo, D.; Romero, L.; Merlos, M.; Vela, J. M. Sigma 1 Receptor: A New Therapeutic Target for Pain. *Eur. J. Pharmacol.* **2013**, *716*, 78–93.

(30) Chien, C. C.; Pasternak, G. W. Functional Antagonism of Morphine Analgesia by (+)-Pentazocine: Evidence for an Anti-opioid Sigma 1 System. *Eur. J. Pharmacol.* **1993**, *250*, R7–R8.

(31) Chien, C. C.; Pasternak, G. W. (–)-Pentazocine Analgesia in Mice: Interactions with a Sigma Receptor System. *Eur. J. Pharmacol.* **1995**, *294*, 303–308.

(32) Chien, C. C.; Pasternak, G. W. Sigma Antagonists Potentiate Opioid Analgesia in Rats. *Neurosci. Lett.* **1995**, *190*, 137–139.

(33) Kim, F. J.; Kovalyshyn, I.; Burgman, M.; Neilan, C.; Chein, C. C.; Pasternak, G. W. Sigma-1 Receptor Modulation of G-Protein-Coupled Receptor Signaling: Potentiation of Opioid Transduction Independent from Receptor Binding. *Mol. Pharmacol.* **2010**, *77*, 695–703.

(34) King, M.; Pan, Y. X.; Mei, J.; Chang, A.; Xu, J.; Pasternak, G. W. Enhanced κ -Opioid Receptor-Mediated Analgesia by Antisense Targeting the Sigma-1 Receptor. *Eur. J. Pharmacol.* **1997**, *331*, R5–R6.

(35) Chien, C. C.; Pasternak, G. W. Selective Antagonism of Opioid Analgesia by a Sigma Receptor System. *J. Pharmacol. Exp. Ther.* **1994**, *271*, 1583–1590.

(36) Cendán, C. M.; Pujalte, J. M.; Portillo-Salido, E.; Montoliu, L.; Baeyens, J. M. Formalin-Induced Pain is Reduced in Sigma 1 Receptor Knockout Mice. *Eur. J. Pharmacol.* **2005**, *511*, 73–74.

(37) Entrena, J. M.; Cobos, E. J.; Nieto, F. R.; Cendán, C. M.; Gris, G.; Pozo, E. D.; Zamanillo, D.; Baeyens, J. M. Sigma-1 Receptors Are Essential for Capsaicin-Induced Mechanical Hypersensitivity: Studies with Selective Sigma-1 Ligands and Sigma-1 Knockout Mice. *Pain* **2009**, *143*, 252–261.

(38) Nieto, F. R.; Cendán, C. M.; Sánchez-Fernández, C.; Cobos, E. J.; Entrena, J. M.; Tejada, M. A.; Zamanillo, D.; Vela, J. M.; Baeyens, J. M. Role of Sigma-1 Receptors in Paclitaxel-Induced Neuropathic Pain in Mice. *J. Pain* **2012**, *13*, 1107–1121.

(39) De La Puente, B.; Nadal, X.; Portillo-Salido, E.; Sánchez-Arroyos, R.; Ovalle, S.; Palacios, G.; Muro, A.; Romero, L.; Entrena, J. M.; Baeyens, J. M.; López-García, J. A.; Maldonado, R.; Zamanillo, D.; Vela, J. M. Sigma-1 Receptor Regulate Activity-Induced Spinal Sensitization and Neuropathic Pain after Peripheral Nerve Injury. *Pain* **2009**, *145*, 294–303.

(40) Cendán, C. M.; Pujalte, J. M.; Portillo-Salido, E.; Baeyens, J. M. Antinociceptive Effects of Haloperidol and its Metabolites in the Formalin Test in Mice. *Psychopharmacology* **2005**, *182*, 485–493.

(41) Entrena, J. M.; Cobos, E. J.; Nieto, F. R.; Cendán, C. M.; Baeyens, J. M.; Del Pozo, E. Antagonism by Haloperidol and its Metabolites of Mechanical Hypersensitivity Induced by Intraplantar Capsaicin in Mice: Role of Sigma-1 Receptors. *Psychopharmacology (Berlin, Ger.)* **2009**, *205*, 21–33.

(42) Díaz, J. L.; Cuberes, R.; Berrocal, J.; Contijoch, M.; Christmann, U.; Fernández, A.; Port, A.; Holenz, J.; Buschmann, H.; Laggner, C.; Serafini, M. T.; Burgueño, J.; Zamanillo, D.; Merlos, M.; Vela, J. M.; Almansa, C. Synthesis and Biological Evaluation of the 1-Arylpyrazole Class of σ_1 Receptor Antagonists: Identification of 4-{2-[5-Methyl-1-

(naphthalen-2-yl)-1H-pyrazol-3-yloxy]ethyl]morpholine (S1RA, E-52862). *J. Med. Chem.* **2012**, *55*, 8211–8224.

(43) Romero, L.; Zamanillo, D.; Nadal, X.; Sánchez-Arroyos, R.; Rivera-Arconada, I.; Dordal, A.; Montero, A.; Muro, A.; Bura, A.; Segalés, C.; Laloya, M.; Hernández, E.; Portillo-Salido, E.; Escriche, M.; Codony, X.; Encina, G.; Burgueño, J.; Merlos, M.; Baeyens, J. M.; Giraldo, J.; López-García, J. A.; Maldonado, R.; Plata-Salamán, C. R.; Vela, J. M. Pharmacological Properties of S1RA, a New Sigma-1 Receptor Antagonist that Inhibits Neuropathic Pain and Activity-Induced Spinal Sensitization. *Br. J. Pharmacol.* **2012**, *166*, 2289–2306.

(44) Lan, Y.; Chen, Y.; Xu, X. Q.; Qiu, Y. L.; Liu, S. C.; Liu, X.; Liu, B.-F.; Zhang, G. S. Synthesis and Biological Evaluation of a Novel Sigma-1 Receptor Antagonist Based on 3,4-dihydro-2(1H)-quinoline Scaffolds as a Potential Analgesic. *Eur. J. Med. Chem.* **2014**, *79*, 216–230.

(45) Glennon, R. A.; Ablordeppay, S. Y.; Ismael, A. M.; El-Ashmawy, M. B.; Fischer, J. B.; Howie, K. B. Structural Features Important for Sigma-1 Receptor Binding. *J. Med. Chem.* **1994**, *37*, 1214–1219.

(46) Glennon, R. A. Pharmacophore Identification for Sigma-1 Receptor Binding: Application of the “Deconstruction–Reconstruction–Elaboration” Approach. *Mini-Rev. Med. Chem.* **2005**, *5*, 927–940.

(47) Diaz, G. J.; Daniell, K.; Leitz, S. T.; Martin, R. L.; Su, Z.; McDermott, J. S.; Cox, B. F.; Gintant, G. A. The [³H]-Dofetilide Binding Assay Is a Predictive Screening Tool for hERG Blockade and Proarrhythmia: Comparison of Intact Cell and Membrane Preparations and Effects of Altering [K⁺]_o. *J. Pharmacol. Toxicol. Methods* **2004**, *50*, 187–199.

(48) (a) Cobos, E. J.; Baeyens, J. M.; Del Pozo, E. Phenytoin Differentially Modulates the Affinity of Agonist and Antagonist Ligands for Sigma-1 Receptors of Guinea Pig Brain. *Synapse* **2005**, *55*, 192–195. (b) Maricel, G. S.; Victor, F. D.; Enrique, P. S.; Pilar, P.; Daniel, Z.; Vela, J. M.; Javier, B.; Francisco, C. Predicting the Antinociceptive Efficacy of σ_1 Receptor Ligands by a Novel Receptor Fluorescence Resonance Energy Transfer (FRET) Based Biosensor. *J. Med. Chem.* **2014**, *57*, 238–242.

(49) Diaz, J. L.; Christmann, U.; Fernández, A.; Luengo, M.; Bordas, M.; Enrech, R.; Carro, M.; Pascual, R.; Burgueño, J.; Merlos, M.; Benet-Buchholz, J.; Cerón-Bertran, J.; Ramírez, J.; Reinoso, R. F.; Fernández de Henestrosa, A. R.; Vela, J. M.; Almansa, C. Synthesis and Biological Evaluation of a New Series of Hexahydro-2H-pyrano[3,2-c]quinolines as Novel Selective σ_1 Receptor ligands. *J. Med. Chem.* **2013**, *56*, 3665–3656.

(50) Bennett, G. J.; Xie, Y. K. A Peripheral Mononeuropathy in Rat that Produces Disorders of Pain Sensation like Those Seen in Man. *Pain* **1988**, *33*, 87–107.

(51) Caspni, O.; Reitz, M. C.; Ceci, A.; Kremer, A.; Treede, R. D. Tramadol Reduced Anxiety-Related and Depression-Associated Behaviors Presumably Induced by Pain in the Chronic Constriction Injury Model of Neuropathic Pain in Rats. *Pharmacol. Biochem. Behav.* **2014**, *124*, 290–296.

(52) Dahlgren, M. K.; Garcia, A. B.; Hare, A. A.; Tirado-Rives, J.; Leng, L.; Bucala, R.; Jorgensen, W. L. Virtual Screening and Optimization Yield Low-Nanomolar Inhibitors of the Tautomerase Activity of *Plasmodium falciparum* Macrophage Migration Inhibitory Factor. *J. Med. Chem.* **2012**, *55*, 10148–10159.

(53) Zanatta, N.; Fantinel, L.; Lourega, R. V.; Bonacorso, H. G.; Martins, M. A. P. A Convenient Synthesis of 5- and 6-Substituted 2-Phenyl-3H-Pyrimidin-4-Ones. *Synthesis* **2008**, *3*, 358–362.

(54) Kato, T.; Yamanaka, H.; Konno, S. Synthesis of 3-Amino-4-methyl-2-pentenamide, 2-Amino-1-clohexene-1-carboxamide, 3-Amino-2,4-diphenyl-2-butenamide, and Synthesis of 4(3H)-Pyrimidone Derivatives From Them. *Yakugaku Zasshi* **1971**, *91* (9), 1004–1012.

(55) Raboisson, P. Jean-Marie B.; Belfrage, A. K.; Gertrud L.; Classon, B. O.; Lindquist, K. C.; Nilsson, K. M.; Rosenquist, A. A. K.; Samuelsson, B. B.; Waehling, H. J. Preparation of Pyrimidine-Substituted Macrocyclic Peptides as Inhibitors of Hepatitis C Virus. *PCT Int. Appl. WO 2008095999 A1 20080814*, 2008.

(56) Guan, H. P.; Hu, Q. S.; Hu, C. M. Synthesis of 2-Substituted 6-fluoroalkylpyrimidin-4(3H)-ones and Pyrimidines. *Synthesis* **1996**, *8*, 997–1001.

(57) (a) Naganuma, K.; Omura, A.; Maekawara, N.; Saitoh, M.; Ohkawa, N.; Kubota, T.; Nagumo, H.; Kodama, T.; Takemura, M.; Ohtsuka, Y. Discovery of Selective PDE4B Inhibitors. *Bioorg. Med. Chem. Lett.* **2009**, *19*, 3174–3176. (b) Grassi, G.; Foti, F.; Risitano, F. Ring-Enlargement of Isoxazol-3-ones to 1,3-Oxazin-4-ones. *J. Chem. Res. Synopses* **1983**, *4*, 102–103.

(58) Hayashi, S.; Masui, A.; Sekiguchi, F. Fluorine-Containing Phosphate Esters of Pyrimidinols as Insecticides and Acaricides, *Jpn. Kokai Tokkyo Koho* 1986, JP 61268694 A 19861128, 1986.

(59) Yoburn, J. C.; Baskaran, S. Chemoselective Arylamidine Cyclizations: Mild Formation of 2-Arylimidazole-4-carboxylic Acids. *Org. Lett.* **2005**, *7*, 3801–3803.

(60) (a) Ho, S. L.; Cho, C. S. Microwave-Assisted Copper-Powder-Catalyzed Synthesis of Pyrimidinones from β -Bromo α,β -Unsaturated Carboxylic Acids and Amidines. *Synlett* **2013**, *24*, 2705–2708.

(b) Goto, T.; Shiina, A.; Yoshino, T.; Mizukami, K.; Hirahara, K.; Suzuki, O.; Sogawa, Y.; Takahashi, T.; Mikkaichi, T.; Nakao, N. Identification of the Fused Bicyclic 4-Amino-2-phenylpyrimidine Derivatives as Novel and Potent PDE4 Inhibitors. *Bioorg. Med. Chem. Lett.* **2013**, *23*, 3325–3328.

(61) Sun, X. J.; Tymianski, M.; Garman, J. D., Agents and Methods for Treating Ischemic and Other Diseases Caused by TRPM7 Gene and Protein Activity. *PCT Int. Appl. WO 2011072275 A2 20110616*, 2011.

(62) (a) Reigan, P.; Gbaj, A.; Stratford, I. J.; Bryce, R. A.; Freeman, S. Xanthine Oxidase-Activated Prodrugs of Thymidine Phosphorylase Inhibitors. *Eur. J. Med. Chem.* **2008**, *43*, 1248–1260. (b) Ataka, K.; Kono, M., Method for The Preparation of 5-Chloro-4-hydroxy-6-methylpyrimidine by Cyclocondensation of 2-Chloro-3-oxobutanoic Ester with Formamidine, *Jpn. Kokai Tokkyo Koho* 1996, JP 08198858 A 19960806, 1996. (c) Zurmuehlen, F., Preparation of 5-Chloro-4-hydroxypyrimidines, *Ger. Offen.* 1995, DE 4323180 A1 19950119, 1995.

(63) Breslin, M. J.; Cox, C. D.; Hartingh, T. J.; Pero, J.; Raheem, I. T.; Rossi, M.; Vassallo, L., Preparation of Aryloxymethylcyclopropane Derivatives As PDE10 Inhibitors, *PCT Int. Appl. WO 2012162213 A1 20121129*, 2012.

(64) Chokai, S.; Aoki, T.; Kimura, K., Preparation and Formulation of Pyrimidine Derivatives As Brain Function Improvers, *PCT Int. Appl.* 1992, WO 9204333 A1 19920319, 1992.

(65) DeHaven-Hudkins, D. L.; Fleissner, L. C.; Ford-Rice, F. Y. Characterization of the Binding of [³H](+)-Pentazocine to Sigma Recognition Sites in Guinea Pig Brain. *Eur. J. Pharmacol.* **1992**, *227*, 371–378.

(66) Bradford, M. M. A Rapid and Sensitive Method for the Quantitation of Microgram Quantities of Protein Utilizing the Principle of Protein–Dye Binding. *Anal. Biochem.* **1976**, *72*, 248–254.

(67) Ronsisvalle, G.; Marrazzo, A.; Prezzavento, O.; Cagnotto, A.; Mennini, T.; Parenti, C.; Scoto, G. M. Opioid and Sigma Receptor Studies. New Developments in the Design of Selective Sigma Ligands. *Pure Appl. Chem.* **2011**, *73*, 1499–1509.